



# Modulation of Hippocampal Network Oscillation by PICK1-Dependent Cell Surface Expression of mGlu3 Receptors

Pola Tuduri,\* Nathalie Bouquier,\*  Benoit Girard,\* Enora Moutin, Maxime Thouaye,  Julie Perroy, Federica Bertaso, and Jeanne Ster

Institut de Génomique Fonctionnelle, University of Montpellier, Centre National de la Recherche Scientifique, Institut National de la Santé et de la Recherche Médicale, Montpellier, 34094, France

Metabotropic glutamate receptor Type 3 (mGlu3) controls the sleep/wake architecture, which plays a role in the glutamatergic pathophysiology of schizophrenia. Interestingly, mGlu3 receptor expression is decreased in the brain of schizophrenic patients. However, little is known about the molecular mechanisms regulating mGlu3 receptors at the cell membrane. Subcellular receptor localization is strongly dependent on protein–protein interactions. Here we show that mGlu3 interacts with PICK1 and that this scaffolding protein is important for mGlu3 surface expression and function in hippocampal primary cultures. Disruption of their interaction via an mGlu3 C-terminal mimicking peptide or an inhibitor of the PDZ domain of PICK1 altered the functional expression of mGlu3 receptors in neurons. We next investigated the impact of disrupting the mGlu3-PICK1 interaction on hippocampal theta oscillations *in vitro* and *in vivo* in WT male mice. We found a decreased frequency of theta oscillations in organotypic hippocampal slices, similar to what was previously observed in mGlu3 KO mice. In addition, hippocampal theta power was reduced during rapid eye movement sleep, non-rapid eye movement (NREM) sleep, and wake states after intraventricular administration of the mGlu3 C-terminal mimicking peptide. Targeting the mGlu3-PICK1 complex could thus be relevant to the pathophysiology of schizophrenia.

**Key words:** hippocampus; interacting proteins; mGlu3; oscillations; PICK1

## Significance Statement

Dysregulation of the glutamatergic system might play a role in the pathophysiology of schizophrenia. Metabotropic glutamate receptors Type 3 (mGlu3) have been proposed as potential targets for schizophrenia. Understanding the molecular mechanisms regulating mGlu3 receptor at the cell membrane is critical toward comprehending how their dysfunction contributes to the pathogenesis of schizophrenia. Here we describe that the binding of the signaling and scaffolding protein PICK1 to mGlu3 receptors is important for their localization and physiological functions. The identification of new proteins that associate specifically to mGlu3 receptors will advance our understanding of the regulatory mechanisms associated with their targeting and function and ultimately might provide new therapeutic strategies to counter these psychiatric conditions.

## Introduction

As the brain major neurotransmitter, glutamate is critical for central nervous system (CNS) function. A number of findings

implicate glutamate as an essential contributing factor for theta oscillations (Buzsaki and Draguhn, 2004; Sohal et al., 2009) and abnormalities in glutamatergic neurotransmission lead to altered network oscillations in all frequency bands. Pathologic alterations of the neurotransmitter systems involved in the generation and synchronization of neural oscillations are believed to be the cause of these perturbations (Uhlhaas and Singer, 2010; Basar, 2013). Evidence indicates that dysfunctional neural oscillations hold a great potential as endophenotype that may underlie deficits of disease (Gandal et al., 2012; Lisman, 2016). Glutamate regulates the CNS through the actions of ionotropic and metabotropic receptors (mGlu). Efforts have been focused on characterizing the clinical implications of targeting these receptors. For example, inhibiting NMDAR signaling induces a syndrome in healthy individuals that includes symptoms associated with schizophrenia (Coyle, 2012). However, excessive direct activation of NMDAR induces epileptic seizures and excitotoxicity-induced neuronal

Received Jan. 10, 2022; revised Sep. 27, 2022; accepted Sep. 30, 2022.

Author contributions: P.T., N.B., B.G., E.M., M.T., F.B., and J.S. performed research; P.T., N.B., F.B., and J.S. analyzed data; P.T., N.B., B.G., J.P., F.B., and J.S. edited the paper; N.B., B.G., J.P., F.B., and J.S. designed research; J.S. wrote the first draft of the paper; J.S. wrote the paper.

This work was supported by Fondation pour la Recherche Médicale EQU202203014705 and European Research Council Grant Agreement 646788. We thank Frederic De Bock for slice culturing; the animal facility (iExplore platform of RAM Montpellier, France) and Yan Chastagnier for technical assistance; Laurent Fagni, Philippe Marin, Jean-Philippe Pin, Vincent Compan, and Emmanuel Valjent for valuable discussions; and Corrado Corti, Corrado Corsi, and GlaxoSmithKline for permission to use mGlu3KO mice.

\*P.T., N.B., and B.G. contributed equally to this work.

The authors declare no competing financial interests.

Correspondence should be addressed to Jeanne Ster at [jeanne.ster@igf.cnrs.fr](mailto:jeanne.ster@igf.cnrs.fr).

<https://doi.org/10.1523/JNEUROSCI.0063-22.2022>

Copyright © 2022 the authors

death (Olney et al., 1991) and cannot be considered as a safe therapeutic avenue. mGluRs finely modulate synaptic transmission by a variety of second messengers. Thus, they represent attractive alternative therapeutic targets for the treatment of psychiatric disorders. In particular, mGlu2/3 receptors, and more specifically mGlu3, have been proposed as potential targets for schizophrenia, Parkinson's disease, drug addiction, and anxiety (Rouse et al., 2000; Corti et al., 2007; Bruno et al., 2017).

The mGlu2/3 are broadly expressed in the CNS where they control synaptic plasticity, LTP and LTD acting mainly at presynaptic sites (Yokoi et al., 1996; Lea et al., 2001). In parallel, they play important postsynaptic functions. mGlu2/3 share most of their pharmacology and have been studied as a homogeneous receptor group. Recently, increasing evidence suggests that postsynaptic mGlu3 receptors display a distinct localization and physiological functions in the CNS compared with the closely related mGlu2 receptor. Postsynaptic mGlu3 receptors induce an LTD of excitatory transmission in PFC, which is prevented by stress (Joffe et al., 2019). We have previously shown their involvement in the modulation of theta rhythms (6–14 Hz) in the CA3 area of the hippocampus, which are altered in a mouse model exhibiting a schizophrenic phenotype (Berry et al., 2018). In the hippocampus, activation of mGlu2/3 promotes the induction of synaptic plasticity by modifying postsynaptic NMDAR function (Trepanier et al., 2013; Rosenberg et al., 2016). mGlu2 receptors modulate primarily extrasynaptic NMDARs, while mGlu3 receptors act on both extrasynaptic and synaptic NMDARs (Rosenberg et al., 2016). These data likely reflect the differential somatodendritic localization of these receptors, with mGlu3 receptors being located to synaptic active sites. Despite this evidence, the molecular mechanisms by which mGlu3 receptors participate in the control of these physiological processes remain largely undetermined.

Interacting proteins are associated with different domains of the receptor, in particular its C-terminal domain, and form a functional scaffold, or “receptosome,” that regulates the cellular targeting and specify their coupling to different signal pathways (Bockaert et al., 2010). For example, the interaction between mGlu1/5 and Homer proteins plays an important role in shaping dendritic spines (Ango et al., 2000) and plasticity (Moutin et al., 2012) as a safeguard of brain physiology (Moutin et al., 2021). Less is known about mGlu3 interactors. Yeast 2-hybrid studies identified Protein Interacting with C Kinase 1 (PICK1), GRIP, and PP2C as specific mGlu3-interacting partner (Hirbec et al., 2002; Flajolet et al., 2003). PICK1 is a promising candidate to study the specific localization and function of mGlu3 receptor because of its high expression in the brain and its synaptic localization. PICK1 PDZ domain binds to a large number of proteins, thus regulating the subcellular localization and surface expression of its PDZ-binding partners (Madsen et al., 2005; Xu and Xia, 2006).

We hypothesize that the binding of PICK1 to mGlu3 receptors could be important for the localization of mGlu3 and might modulate its physiological functions.

## Materials and Methods

**Plasmids and peptides.** The pRK5 HA-mGlu3 rat cDNA was a kind gift of Jean-Philippe PIN (Institut de Génétique Fonctionnelle). The plasmid encoding mGlu3 $\Delta$ PDZlig was obtained from the pRK5 HA-mGlu3WT cDNA. The C-terminal sequence TSSL was replaced by a stop codon and a BamHI restriction site by site-directed mutagenesis using the following primers: 5'-CTGGACTCCACCTGAGGATCC TTGTGATACGCAGTTCA-3' and TCGGTATCACAA GGATCC TCA

GGTGGAGTCCAGGACTTC. The GFP-PICK1 cDNA was a kind gift of Oussama El Far (UNIS). The mGlu3-SSL and -SSD peptides for pull-down experiments were synthesized by Eurogentec, with a purity > 70%. The sequence of the mGlu3-SSD peptide was AA AQN LYF QGP QKN VVT HRL HLN RFS VSG TAT TYS QSS AST YVP TVC NGR EVL DST TSS D, and the sequence of the mGlu3-SSL peptide was AA AQN LYF QGP QKN VVT HRL HLN RFS VSG TAT TYS QSS AST YVP TVC NGR EVL DST TSS L.

TAT mGlu3 peptides for *ex vivo* and *in vivo* applications were synthesized with a purity > 95% (Eurogentec) with the following sequences: TAT-control peptide: YGR KKR RQR RRE VLD AAA; TAT-mGlu3 peptide: YGR KKR RQR RRE VLD SSL. Both peptides were diluted to 1 or 10  $\mu$ M in the appropriate media depending on the type of experiment.

The TAMRA-tagged TAT-mGlu3 peptide was synthesized by Smart Bioscience, with a purity > 95%. The sequence of TAMRA TAT-mGlu3 peptide was TAMRA-YGR KKR RQR RRE VLD SSL.

**Drugs.** LCCG-1 D-AP5, methacholine chloride (MCh), and TTX were purchased from Tocris Bioscience and FSC231 from Sigma-Aldrich. FSC231 was first dissolved in DMSO and then added to the saline solutions (DMSO final concentration < 0.001%).

**HEK cell culture and transfection.** HEK-293 cells were cultured in complemented DMEM as previously described (Perroy et al., 2008). Cells were transfected at 40%–50% confluence using polyethylenimine (Polysciences) (Dubois et al., 2009) and used 24 h after transfection.

**Hippocampal primary cultures and transfection.** Postnatal neuronal cultures were prepared from WT C57Bl6/J pups (P0–P2) of both sexes as previously described (Moutin et al., 2020). All animal studies were ethically reviewed and conducted in accordance with European Directive 2010/63/EEC and the University Policy on the Care (protocol approved by the veterinary Department of Animal Care of Montpellier). Briefly, hippocampi were mechanically and enzymatically dissociated with papain (Sigma-Aldrich) and hippocampal cells were seeded in Neurobasal-A medium (Invitrogen) supplemented with B-27 (Invitrogen), Glutamax (Invitrogen), L-glutamine (Invitrogen), antibiotics (Invitrogen), and FBS (Invitrogen). After 2 d in culture, cytosine  $\beta$ -D-arabino-furanoside hydrochloride (Sigma-Aldrich) was added to curb glia proliferation. The day after, 75% of the medium was replaced by BrainPhys medium (Stem Cell Technologies) supplemented with B-27 (Invitrogen), Glutamax (Invitrogen), and antibiotics (Invitrogen). Neurons were cotransfected with the indicated plasmids (HA-mGlu3, HA-mGlu3 $\Delta$ PDZlig, GFP-PICK1, GFP) by using Lipofectamine at DIV10.

**Coimmunoprecipitation experiments.** HEK-293 cells were solubilized in a buffer containing 50 mM Tris HCl, pH 7.4, 100 mM NaCl, 2 mM EDTA, Triton 1%, 2 mM DTT, 2 mM MgCl<sub>2</sub>, and a protease inhibitor cocktail (Roche). Samples (1 mg) were incubated with GFP-Trap beads (Chromotek) or anti-HA antibody Sepharose beads (Sigma-Aldrich, A2095) for 1 h at 4°C. Beads were washed 5 times with 50 mM Tris HCl, pH 7.4, 250 mM NaCl, 2 mM EDTA, Triton 1%, 2 mM DTT, 2 mM MgCl<sub>2</sub>, and immunoprecipitated proteins were analyzed by Western blotting.

**Pull-down experiments.** The mGlu3-SSL or -SSD peptides were coupled to activated CnBr-Sepharose 4B (GE Healthcare) according to the manufacturer's instructions. Hippocampi from male C57BL/6 mice (Janvier Labs) were extracted, homogenized in lysis buffer containing 50 mM Tris HCl, pH 7.4, 100 mM NaCl, 2 mM EDTA, Triton 1%, 2 mM DTT, 2 mM MgCl<sub>2</sub> and a protease inhibitor cocktail (Roche) using a Potter homogenizer, and then centrifuged at 10,000  $\times$  g for 10 min. Solubilized proteins (10 mg per condition) were incubated at least 2 h with or without the TAT-conjugated peptide of interest before incubation overnight at 4°C with immobilized C terminal peptide. Samples were washed twice with 5 ml of extraction buffer containing 500 mM Tris-EDTA, 250 mM NaCl, pH 8, and then twice with high sodium extracting buffer containing 500 mM Tris-EDTA, 500 mM NaCl, pH 8, before elution in SDS sample buffer. Samples were analyzed by Western blotting.

**Western blot.** Protein concentration in each lysate was determined by the bicinchoninic acid method. Proteins were resolved on 10% acrylamide gels and transferred electrophoretically onto nitrocellulose membranes (GE Healthcare). Membranes were incubated in blocking buffer

containing the following: PBS 0.1% Tween-20, and 5% skimmed dried milk for 1 h at room temperature and overnight with primary antibodies in blocking buffer: chicken anti-PICK1 (1:500, NBP1-42 829, Novus Biologicals), rat anti-HA (1:500, 11867423001, clone 3F10; Roche), or monoclonal mouse anti-GFP antibody (1:1000, Clontech catalog #632381). Membranes were then washed and incubated with HRP-conjugated anti-chicken, anti-mouse, or anti-rat secondary antibodies (1:4000 in blocking buffer, GE Healthcare) for 1 h at room temperature. Immunoreactivity was detected with an enhanced chemiluminescence method (enhanced chemiluminescence detection reagent, GE Healthcare). Immunoreactive bands were quantified by densitometry using the ImageJ software (National Institutes of Health).

**Endocytosis experiments.** Receptor internalization was evaluated using a fluorescence-based antibody-uptake assay described previously (Lavezzari et al., 2004). Briefly, transfected neurons (DIV12) were incubated with anti-HA primary antibody (rat monoclonal antibody, clone 3F10; Roche) for 1 h at 4°C to label surface-expressed mGlu3 receptors and then returned to conditioned media for 15 min at 37°C, enabling endocytosis of cell-surface mGlu3 receptors bound to rat anti-HA antibody. Then, cells were fixed and incubated with anti-rat biotin-conjugated secondary antibody (Jackson ImmunoResearch Laboratories, catalog #112-066-006) and CF350-streptavidin (blue; Biotium, catalog #29031) to label the surface population of receptors. We decided to use a biotin-conjugated secondary antibody to amplify the signal in CF350 (blue), which enables us to increase the signal-to-noise ratio and thus make a better detection of membrane receptors. Next, the cells were permeabilized and then incubated with an anti-rat Cy3-conjugated (red, Jackson ImmunoResearch Laboratories, catalog #712-165-150) secondary antibody to label the internalized population of receptors. The cells were mounted with Mowiol and imaged on an epifluorescent microscope equipped for optical sectioning (AxioImager Z1 Zeiss microscope equipped for optical sectioning Apotome, Carl Zeiss). Internalization was assessed in at least three independent experiments for each condition.

The fluorescence intensity (pixels) is measured on each channel (CY3 values: endocytosis; CF350: membrane) in a specific location (ROI) using the Image J software (National Institutes of Health). The ratio between the fluorescence intensity value of the CF350 channel and the CY3 channel is calculated. One ROI per neuron was collected, and colocalization analysis was measured based on the data collected in three independent experiments (at least 6–20 neurons/condition).

**Biotinylation experiments.** Acute hippocampal slices (350  $\mu$ m) were prepared from adult male C57BL/6J mice in ice-cold dissection buffer maintained in 5% CO<sub>2</sub>/95% O<sub>2</sub> and containing the following (in mM): 25 NaHCO<sub>3</sub>, 1.25 NaH<sub>2</sub>PO<sub>4</sub>, 2.5 KCl, 0.5 CaCl<sub>2</sub>, 7 MgCl<sub>2</sub>, 25 D-glucose, 110 choline chloride, 11.6 ascorbic acid, 3.1 pyruvic acid. Slices were then transferred to aCSF (composition in mM as follows: 124 NaCl, 3 KCl, 26 NaHCO<sub>3</sub>, 1.25 NaH<sub>2</sub>PO<sub>4</sub>, 2 CaCl<sub>2</sub>, 1 MgCl<sub>2</sub>, 10 D-glucose, saturated with 95% O<sub>2</sub> and 5% CO<sub>2</sub>). Slices were maintained on filters in a submersion storage chamber and allowed to recover for at least 1 h before use. Four or five individual slices were used per condition and incubated with different treatments (FSC231 25  $\mu$ M, 1 h; TAT 10  $\mu$ M, 1 h). Slices were washed once with ice-cold aCSF (5 min) and then incubated with 0.5 mg/ml EZ-link sulfo-NHS-SS-Biotin (Pierce) for 30 min on ice before four washes in aCSF supplemented with ethanolamine, pH 7.4 (50 mM/5 min), to quench free reactive biotin. Tissue lysis was then performed using a Potter homogenizer followed by incubation 30 min at 4°C in cell lysis buffer (100 mM NaCl, 20 mM Tris HCl, pH 7.4, 5 mM EDTA, 1% Triton X-100) mixed with protease inhibitors. Samples were centrifuged at 16,000  $\times$  g for 20 min at 4°C, and the protein concentration of the resulting supernatants was determined using a BCA kit (Sigma). A fraction of the lysate (30  $\mu$ g of proteins) was kept as a whole input (total) reference sample. Biotinylated proteins were purified by pull down on equilibrated Neutravidin-coated magnetic beads (Spherotech) overnight at 4°C on shaker. Beads were subsequently washed 3 times with lysis buffer, and biotinylated proteins were eluted in 4 $\times$  SDS-PAGE denaturing buffer (Bio-Rad) supplemented with 10%  $\beta$ -mercaptoethanol and heated for 5 min at 60°C. Total and surface mGlu3 expressions as well as actin control were analyzed by Western blot with specific antibodies (anti-mGlu3: Abcam #ab166608; anti-Actin: Sigma #A5441).

**Organotypic hippocampal slices.** Organotypic hippocampal slices were prepared from 6-d-old WT C57BL/6J and mGlu3 KO mice pups as previously described (Stoppini et al., 1991). All animal studies were ethically reviewed and conducted in accordance with European Directive 2010/63/EEC and the University Policy on the Care (protocol approved by the veterinary Department of Animal Care of Montpellier). Three to five mice were used for each slice culture preparation, and each experimental condition was tested over the course of at least three preparations. Slices were placed on a 30 mm porous membrane (Millipore) and kept in 100-mm-diameter Petri dishes filled with 5 ml of culture medium containing 25% heat-inactivated horse serum, 25% HBSS, 50% Opti-MEM, penicillin 25 units/ml, and streptomycin 25  $\mu$ g/ml (Invitrogen). Cultures were maintained in a humidified incubator at 37°C and 5% CO<sub>2</sub> until DIV3 and then were kept at 33°C and 5% CO<sub>2</sub> until the electrophysiological experiments.

**Electrophysiology.** After 3 weeks *in vitro*, slices cultures were transferred to a recording chamber on an upright microscope (Olympus). Slices were superfused continuously at 1 ml/min with a solution containing the following (in mM): 125 NaCl, 2.7 KCl, 11.6 NaHCO<sub>3</sub>, 0.4 NaH<sub>2</sub>PO<sub>4</sub>, 1 MgCl<sub>2</sub>, 2 CaCl<sub>2</sub>, 5.6 D-glucose, and 0.001% phenol red (pH 7.4, osmolarity 305 mOsm) at 33°C. Whole-cell recordings were obtained from cells held at  $-70$  mV using a Multiclamp 700B amplifier (Molecular Devices). Recording electrodes made of borosilicate glass had a resistance of 4–6 M $\Omega$  (Warner Instruments) and were filled with the following (in mM): 125 K-gluconate, 5 KCl, 10 HEPES, 1 EGTA, 5 Na-phosphocreatine, 0.07 CaCl<sub>2</sub>, 2 Mg-ATP, and 0.4 Na-GTP (pH 7.2, osmolarity 310 mOsm). Membrane potentials were corrected for junction potentials. Pyramidal neurons and interneurons have been distinguished by their location (stratum pyramidale vs stratum oriens/stratum radiatum) and their electrophysiological characteristics (firing rate, resting potential) (Pelkey et al., 2017). For all recording conditions, only cells with access resistance <18 M $\Omega$  and a change of resistance <25% over the course of the experiment were analyzed. Data were filtered with a Hum Bug (Quest Scientific), digitized at 2 kHz (Digidata 1444A, Molecular Devices), and acquired using Clampex 10 software (Molecular Devices).

Activation of mGlu3 receptor by LCCG-1 (10  $\mu$ M) induces an inward current in CA3 pyramidal cells (PCs) in the presence of TTX (1  $\mu$ M), D-AP5 (40  $\mu$ M), and picrotoxin (100  $\mu$ M) (Ster et al., 2011). Methacholine (500 nM; 10–20 min) induces synaptic theta activity in CA3 PCs of hippocampal slice cultures (Fischer et al., 1999). We incubated the hippocampal slice culture with different treatments (FSC231 25  $\mu$ M, 30 min; TAT 1  $\mu$ M, 1 h incubation). For the TAT experiments, TAT peptides (1  $\mu$ M) were also added in the intracellular solution.

**EEG/EMG recording and peptides administration.** WT C57BL/6J mice (10–12 weeks old) were implanted for EEG and EMG recording and intraventricular peptide administration. All the procedures were conducted in accordance with the European Communities Council Directive (authorization APAFIS #19302-2019012516391230 v2 by the French Ministry of Higher Education, Research and Innovation). Mice were housed in groups of 5 per cage until surgery, and maintained in a 12 h light/dark cycle (lights on 7:30 A.M. to 7:30 P.M.), in stable conditions of temperature (22  $\pm$  2°C) and humidity (60%), with food and water provided *ad libitum*.

For surgery, animals were anesthetized with a mix of ketamine (100 mg/kg, Imalgene 500) and xylazine (10 mg/kg, Rompun 2%) plus a local subcutaneous injection of lidocaine (Xylocaine, AstraZeneca; 4 mg/kg in 50  $\mu$ l of sterile 0.9% NaCl solution). They were then placed in a stereotaxic frame using the David Kopf mouse adaptor. A bipolar tungsten Teflon-isolated torsade electrode was placed in the CA3 area of the left dorsal hippocampus (AP =  $-1.85$ , ML = 2.3, DV =  $-1.4$  mm from bregma, <https://scalablebrainatlas.incf.org>). A 4 mm, 26 G canula guide (Phymep) was set into the left ventricle (AP = 0.1, ML = 0.75, DV =  $-2$  mm from bregma). Skull cortical electrodes were placed on the frontoparietal bone and a reference electrode on the occipital bone. Two stainless-steel EMG wires were placed in the neck muscles. All electrodes and the canula were fixed on the skull with dental acrylic cement. After surgery, mice were individually housed to minimize the chances of reciprocal injury caused by snatching of the implants. Freely moving animals were put into individual



Plexiglas boxes, and their microconnectors were plugged to an EEG pre-amplifier circuit close to the head and to the EEG amplifier (Pinnacle Technology). Mice were allowed 1 h 30 to habituate to the new environment and to the injection equipment (injection canula and tubing). We performed a single TAT peptide intracerebroventricular infusion. The presence of this type of peptides in the brain is transient, as they are readily eliminated by the circulation. We have chosen the time window of 10–35 min based on our previous experience with a closely related peptide targeting mGlu7, for which the peak of activity was observed ~20–30 min after infusion (Bertaso et al., 2008). All EEG recordings were performed during the light period (light ON 7:00 A.M., light OFF 7:00 P.M., between 10:00 A.M. and 12:00 P.M.). TAT peptides were delivered via a pump operating a micro-syringe (injection volume: 5  $\mu$ l, 500  $\mu$ M in 0.9% NaCl, 750 nl/min). The electrical activity was recorded and filtered at 4 Hz, sampled at 200 Hz, and recorded by a computer equipped with Sirenia software (Pinnacle Technology). The EMG signal was filtered and sampled at 100 Hz. EEG recordings were performed together with video monitoring of the animal behavior. Sleep scoring and periodograms of the EEG recordings were obtained using Neuroscore (DSI). Awake, non-rapid eye movement (NREM), and rapid eye movement (REM) periods were scored and verified by combining video and EMG signal observations. Power spectra were extracted at the corresponding times for each episode and averaged for the 30 min before and 10–35 min after the infusion (10 min were allowed for peptide diffusion). Power spectral density was calculated using FFT with 2 s temporal and 0.5 Hz frequency resolutions.

**Immunohistochemistry.** Mice were anesthetized using Euthazol and transcardially perfused with 4% PFA followed by 24 h of post-fixation in 4% PFA. Thirty- $\mu$ m-thick slices were incubated in PBS-T (0.5% Triton) with BSA (3%) for 1 h and with the primary antibody (mouse anti-NeuN, Millipore, 1:1000 dilution) for 12 h. Slices were then incubated for 2 h with a secondary antibody (AlexaFluor-488 anti-mouse 1:1000 dilution) and DAPI (1:10000 dilution). Acquisition was performed on an epifluorescence microscope (AxioImager Z1 Zeiss microscope equipped for optical sectioning Apotome, Carl Zeiss). Laser power and detector sensitivity were kept constant for each staining to allow comparison between samples. At least three slices per animal were processed and images analyzed using ImageJ software (<https://imagej.nih.gov/ij/index.html>).

**Statistical data analysis.** GraphPad Prism was used for statistical analyses. Values are mean  $\pm$  SEM. For experiments with two groups, normality of data distribution was determined via the Shapiro–Wilk test. Except where noted, normally distributed data were analyzed via *t* tests. For datasets with non-normal distributions, nonparametric tests were used (Mann–Whitney *U* test or Kruskal–Wallis test for independent samples or Wilcoxon signed-rank test for paired samples). For multiple comparisons (see Figs. 1, 2, 3C, 4B, 5A, 6D, 7D, 8D), one-way ANOVA followed by Tukey's multiple comparisons test was used. In Figure 9, spectral analysis was analyzed via two-way ANOVA follow by Tukey's multiple comparisons tests and, for the histograms, via a Kruskal–Wallis analysis (multiple pairwise comparisons followed by Dunn's *post hoc* test).

Oscillation analyses were performed after 9 min of application of LCCG-1 or MCh. Calculation of oscillatory activity was performed from the time of the second peak in the Clampfit autocorrelation function. A segment was considered rhythmic when the second peak of the autocorrelation function was at least 0.3 and several regularly spaced peaks appeared (Ster et al., 2011).

## Results

### The mGlu3 receptor interacts with PICK1

To characterize the interaction between PICK1 and mGlu3 receptor, we first used a coimmunoprecipitation approach. We transiently expressed a GFP-tagged PICK1 (GFP-PICK1) in the absence or presence of mGlu3 receptor bearing an HA tag in the extracellular N-terminal domain of the receptor (HA-mGlu3) in HEK-293 cells and performed coimmunoprecipitation experiments using a GFP nanobody (Fig. 1A). We detected

bands of stronger intensity ~200 kDa/100 kDa corresponding to mGlu3 dimers/monomers in the presence of HA-mGlu3 and GFP-PICK1, compared with cells expressing HA-mGlu3 and GFP. As PICK1 contains a single PDZ domain that could interact with the PDZ ligand motif of mGlu3 receptors, we generated a truncated mGlu3 mutant lacking its “-SSL” PDZ ligand motif, HA-mGlu3 $\Delta$ PDZlig. Deletion of the last three amino acids in the distal C-terminal of mGlu3 receptors (HA-mGlu3 $\Delta$ PDZlig) significantly reduced the coimmunoprecipitation between mGlu3 and PICK1 (Fig. 1A). This result indicates that the PDZ-ligand motif of mGlu3 receptor is necessary for its interaction with PICK1. We confirmed this interaction by performing a reverse immunoprecipitation using anti HA- antibody (Fig. 1B). We observed a trend toward decreased PICK1 binding to the truncated mGlu3 receptor. Given the high sequence homology of mGlu2 and mGlu3 receptor C-terminal sequences, we addressed the specificity of the interaction of PICK1 with mGlu3 receptor by performing a similar coimmunoprecipitation approach as in Figure 1A using an HA-tagged mGlu2 (HA-mGlu2) construct (Fig. 1C). No band was detected in cells transfected with HA-mGlu2 and GFP-PICK1, indicating that PICK1 interacts with mGlu3 but not mGlu2, despite the identical PDZ binding motif.

To further demonstrate a direct interaction between mGlu3 and PICK1, we conducted pull-down experiments of cytosolic PICK1 with synthetic peptides encompassing the C-terminal domain of the mGlu3 receptor conjugated to Sepharose beads. Two different synthetic peptides were generated: one corresponding to the last 60 amino acids in the C-terminal of mGlu3 receptor (mGlu3R3ctWT) and a similar peptide in which the C-terminal leucine was replaced by a glutamate (mGlu3R3ctSSD), to hinder the interaction. Lysates of cells expressing or not PICK1 were incubated with these peptides (Fig. 2A). As expected, we detected a stronger interaction with GFP-PICK1 when using mGlu3R3ctWT beads (~75 kDa band, detected with both anti-GFP and anti-PICK1 antibodies) consistent with a direct interaction between mGlu3 and PICK1. We then tested the mGlu3R3ctWT and mGlu3R3ctSSD beads on mouse hippocampi lysates (Fig. 2B). The mGlu3 C-terminal coimmunoprecipitated with the native PICK1 (50 kDa) expressed in mice brain, indicating that they may form a complex. We also found that the mutant bearing a point of mutation in the ligand PDZ domain (mGlu3R3ctSSD) tended to decrease the interaction with PICK1. Together, these results show that mGlu3 directly interacts specifically via its C terminal to the PDZ domain of endogenous PICK1.

### Peptidic and pharmacological tools to uncouple binding of mGlu3 to PICK1

To determine the functional role of the mGlu3-PICK1 coupling, we used and engineered tools to disrupt their interaction. First, we designed a competitive peptide encompassing the last 10 C-terminal amino acids of the mGlu3 receptor, which included the PDZ ligand motif SSL, conjugated to the cell-membrane transduction domain of the HIV-1 Tat protein (TAT-mGlu3, Fig. 3A). A control peptide was prepared bearing the same overall sequence with the exception of the last three amino acids of the PDZ ligand motif, SSL, which were mutated to alanine (AAA). To evaluate the binding of PICK1 to mGlu3 receptors in the presence of the TAT-mGlu3, we used a coimmunoprecipitation approach as in Figure 1A (see Fig. 3B). There was a strong reduction in the intensity of band corresponding to the receptor (~200 kDa) in cells cotransfected with HA-mGlu3 and GFP-PICK1 in the presence of TAT-mGlu3 compared with TAT-control.

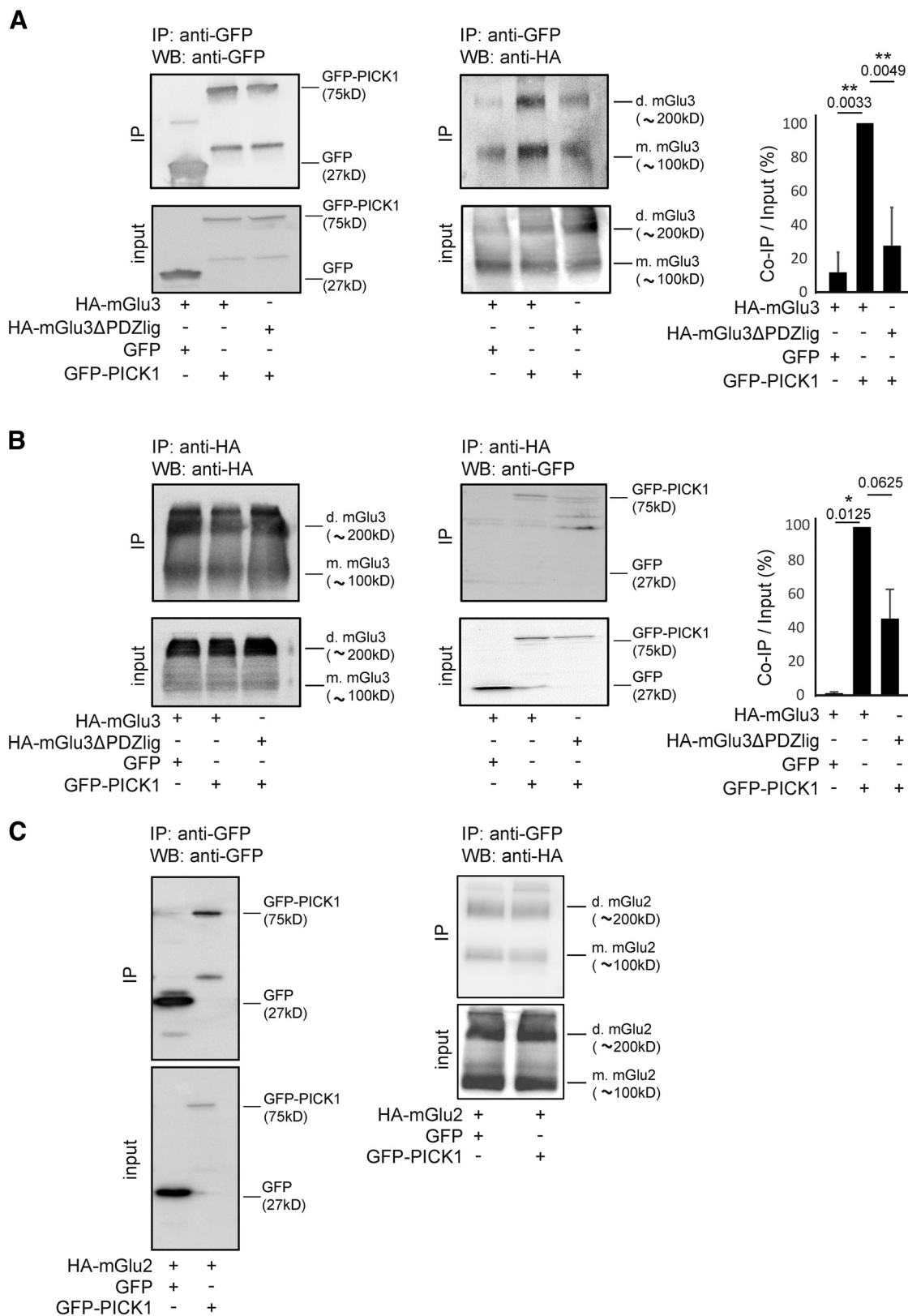


**Figure 1.** Specific interaction of HA-mGlu3 receptor with GFP-PICK1 in HEK-293 cells. HEK-293 cells were transfected with plasmids encoding either HA-mGlu3 or HA-mGlu3ΔPDZlig and cotransfected with GFP-PICK1 or GFP. Proteins were immunoprecipitated with either GFP-Trap beads (**A**) or monoclonal anti-HA antibody (**B**). mGlu3 receptor and PICK1 expression in inputs and immunoprecipitates were analyzed by Western blotting using anti-HA and anti-GFP antibody, respectively. Histogram represents the amount of mGlu3/PICK1 binding (IP/Input ratio; **A**: quantification WB anti-HA, **B**: quantification WB anti-GFP). Results are mean ± SEM for densitometry analyses of blots obtained in three independent experiments performed on different sets of cultured cells. **C**, HA-tagged mGlu2 receptors coexpressed with GFP-PICK1 or GFP alone were immunoprecipitated using anti-HA agarose antibody and detected using an anti-GFP antibody. **C**, Representative of two independent experiments. Mw, Molecular mass (indicated in kDa); IP, immunoprecipitation; d.mGlu3, dimer mGlu3; m.mGlu3, monomer mGlu3. Data are mean ± SEM. \**p* < 0.05. \*\**p* < 0.01.

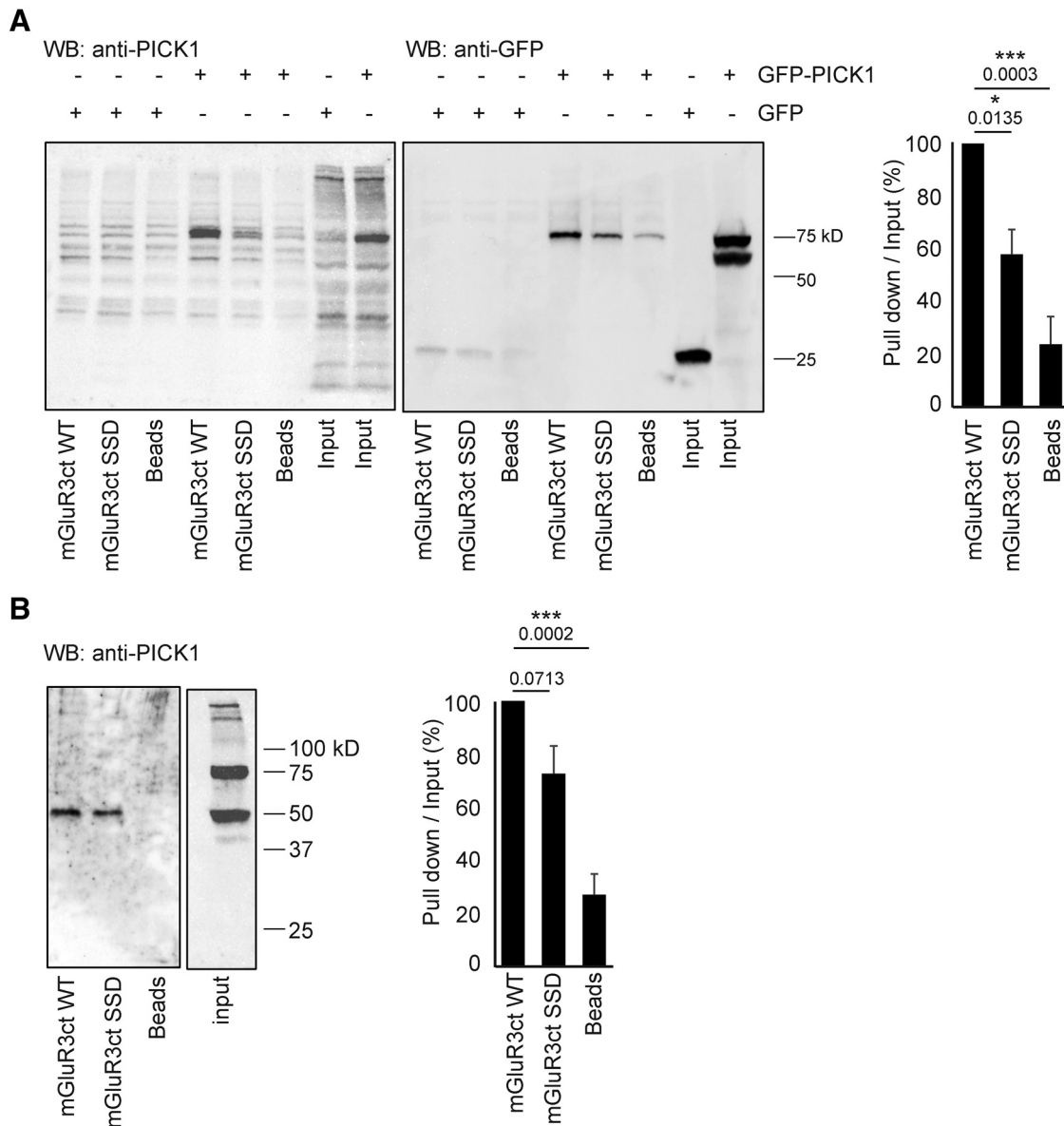


**Figure 2.** The mGlu3 C-terminus associates with native PICK1. **A**, HEK lysates expressing GFP-PICK1 or GFP were incubated with Sepharose-immobilized synthetic peptides that incorporated either the 20 C-terminal residues of the WT (mGlu3RctWT) or mutated mouse mGlu3 receptor (mGlu3ctSSD) or with Sepharose beads only. **B**, Protein extracts from mouse brain were incubated with the indicated Sepharose-immobilized peptides, and bound proteins were analyzed by Western blotting with an anti-PICK1 antibody. Native PICK1 expressed in mice brain coimmunoprecipitates with the mGlu3 receptor C-terminal. Representative data of three independent experiments are illustrated. Data are mean  $\pm$  SEM. \* $p < 0.05$ . \*\*\* $p < 0.001$ .

To confirm the specificity of the TAT-mGlu3 to mGlu3 receptor, we performed a similar coimmunoprecipitation targeting the mGlu7 receptor, which also interacts with PICK1 (Hirbec et al., 2002) (Fig. 3C). We observed that binding of PICK1 to the mGlu7 receptor was prevented by neither peptide. The specificity of the TAT peptides was further characterized by pull-down experiments. We detected a dose-dependent decrease in native PICK1 binding to mGlu3 only when TAT-mGlu3 was added to the mouse brain lysate (Fig. 3D). Together, these data confirmed the specific competition between TAT-mGlu3 and mGlu3 for its receptors. The second strategy was to perform coimmunoprecipitation experiments using a small PICK1 PDZ-binding molecule, FSC231, which is known to prevent PICK interactions (Thorsen et al., 2010). This compound altered the binding of PICK1 to mGlu3 receptor compared with the control (DMSO, Fig. 3E).

#### PICK1 regulates mGlu3 receptor surface expression via the PDZ ligand motif

Membrane protein localization depends on interactions with intracellular binding partners. We tested whether this was the case for mGlu3 receptor and PICK1, first in the heterologous expression system HEK293 cells. We monitored the constitutive trafficking of an HA-tagged version of the receptor together with either GFP-PICK1 or GFP (Fig. 4A). We visualized HA antibody-labeled surface receptors before permeabilization (CF350-streptavidin) and internalized receptors after permeabilization (Cy3 tagged secondary antibody). When transfected with GFP, the receptor was diffusely distributed throughout the cell (ratio surface vs cytoplasm =  $1.64 \pm 0.08$ ). Internalized mGlu3 receptors formed clusters in the cytoplasm. By contrast, when the receptor was cotransfected with GFP-PICK1, surface expression of HA-mGlu3 was significantly increased (ratio surface

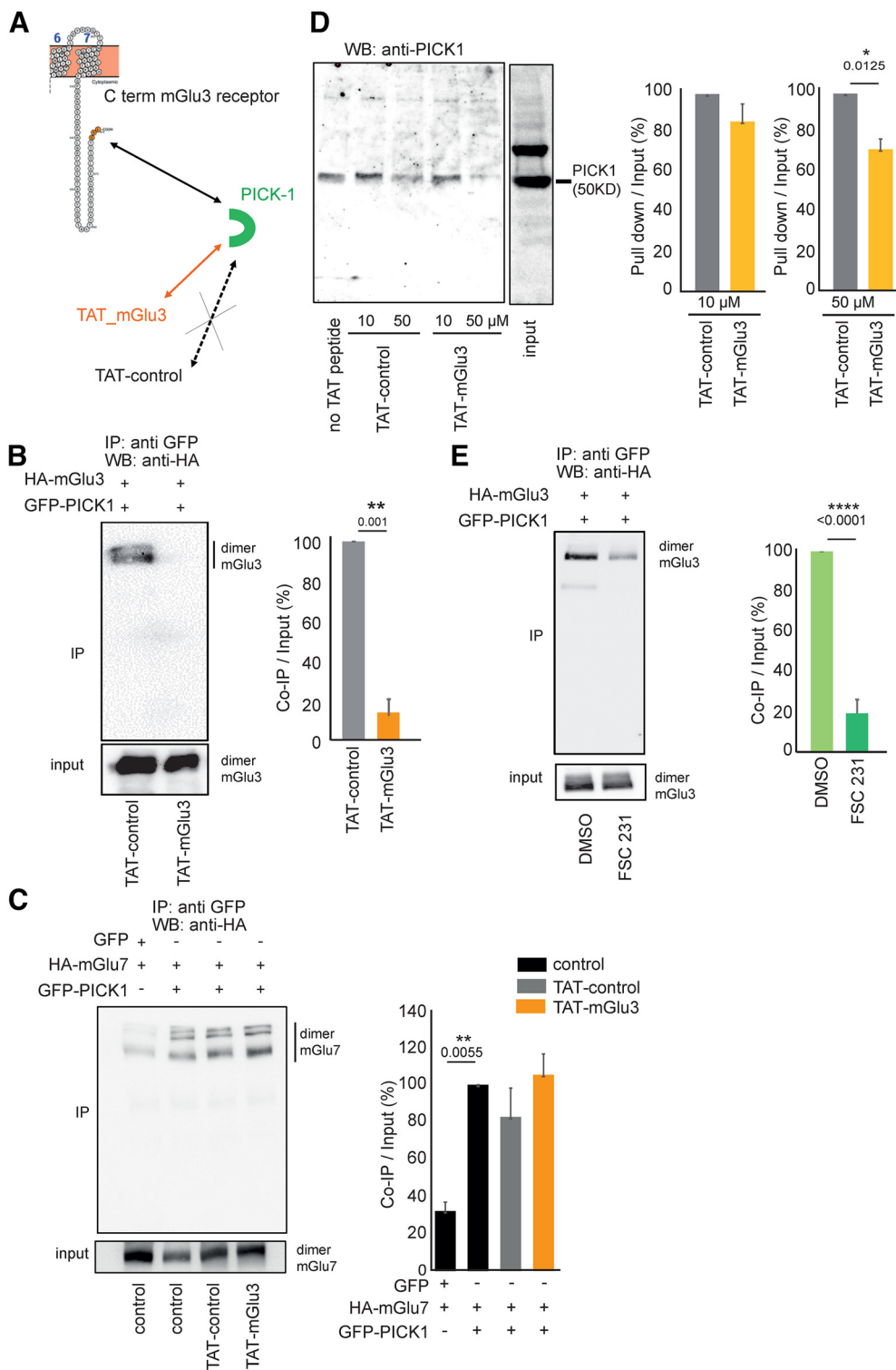


**Figure 3.** Pharmacological tools uncoupling mGlu3 PICK1 interaction *in vitro*. **A**, Schematic representation of the action of TAT peptides on PDZ interaction with mGlu3 C-terminal. Coimmunoprecipitation of HA-mGlu3 (anti-HA antibody) and PICK1 from HEK-293 lysates with either no drug, with TAT peptides (10  $\mu$ M each; **B**), FSC231 (25  $\mu$ M) or DMSO (25  $\mu$ M; **E**). HEK-293 cells were cotransfected with plasmids encoding HA-mGlu3 and GFP-PICK1. Proteins were immunoprecipitated with GFP-Trap beads. Total protein extracts were analyzed by Western blotting using anti-HA antibody. **C**, HA-tagged mGlu7 receptor coexpressed with GFP-PICK1 or GFP alone was immunoprecipitated using GFP-Trap beads and detected using an anti-HA antibody. **D**, Pull-down experiment conducted using mouse brain extracts supplemented with no TAT peptide, 10 or 50  $\mu$ M TAT-control peptide, and 10 or 50  $\mu$ M TAT-mGlu3 peptide. **B–E**, Representative of three independent experiments. **B**, **C**, **E**, Histograms represent the amount of mGlu3-PICK1 binding. Results are mean  $\pm$  SEM for densitometry analyses of blots obtained in three independent experiments performed on different sets of cultured cells. \* $p$  < 0.05, \*\* $p$  < 0.01, \*\*\*\* $p$  < 0.0001.



vs cytoplasm =  $2.32 \pm 0.28$ ). Moreover, most of the internalized receptors were located near the cell membrane. These results indicated that the localization of mGlu3 receptors depends on PICK1 expression in HEK-293 cells.

To deepen this characterization, we studied the localization of mGlu3 and PICK1 in primary hippocampal neurons and found similar results to those observed in HEK-293 cells (Fig. 4B). In neurons cotransfected with HA-mGlu3 and GFP-PICK1, surface levels of mGlu3 receptors were higher than in neurons transfected with HA-mGlu3 alone. Previous studies have shown that the PDZ ligand residues of the intracellular C terminus of mGluRs are critical for their synaptic localization (Boudin et al., 2000). We tested whether the PDZ ligand also plays a role in mGlu3 receptor endocytosis. The surface expression of the HA-mGlu3 $\Delta$ PDZlig receptor lacking the PDZ ligand motif was significantly decreased compared with the WT receptor (Fig. 4B; ratio surface/internalized: GFP-PICK1/HA-mGlu3 =  $1.84 \pm 0.15$ ; GFP/HA-mGlu3 =  $1.43 \pm 0.18$ ; GFP-PICK1/HA-mGlu3 $\Delta$ PDZlig =  $0.95 \pm 0.04$ ).

### Binding to PICK1 is essential for the functional expression of the mGlu3 receptor

We reasoned that an alteration of mGlu3-PICK1 interaction could alter the subcellular localization of the receptors. We examined the effect of an acute treatment with TAT-mGlu3 (1 h at  $1 \mu\text{M}$ ; Fig. 5A,B) or FSC231 (1 h at  $25 \mu\text{M}$ ; Fig. 5C,D) on the subcellular localization of mGlu3 receptors in neurons. Both treatments induced a significant reduction in mGlu3 receptor surface expression (Fig. 5B,D; ratio surface/internalized: TAT-control =  $1.16 \pm 0.06$ ; TAT-mGlu3 =  $1 \pm 0.03$ ; DMSO =  $1 \pm 0.03$ ; FSC231 =  $0.84 \pm 0.06$ ). Conversely, no significant effect was induced by the TAT-control peptide (Fig. 5).

To confirm that PICK-1 promotes the expression of endogenous receptors at the neuronal membrane, we tagged surface proteins via biotin labeling in hippocampal acute slices after treatment with FSC-231 or the TAT-mGlu3 (Fig. 6). Both treatments induced a significant reduction in mGlu3 receptor surface expression (Fig. 6; purified cell surface fractions of mGlu3 receptors are normalized to the total mGlu3 receptor). Conversely, no significant effect was induced by the TAT-control peptide (Fig. 6). Together, these results show that PICK1 promotes the expression of mGlu3 receptors at the neuronal membrane.

Next, to determine the physiological significance of the mGlu3-PICK1 interaction, we performed patch-clamp recording of CA3 PCs and interneurons in organotypic hippocampal slice cultures in the presence of TAT-mGlu3 peptide or FSC231. As

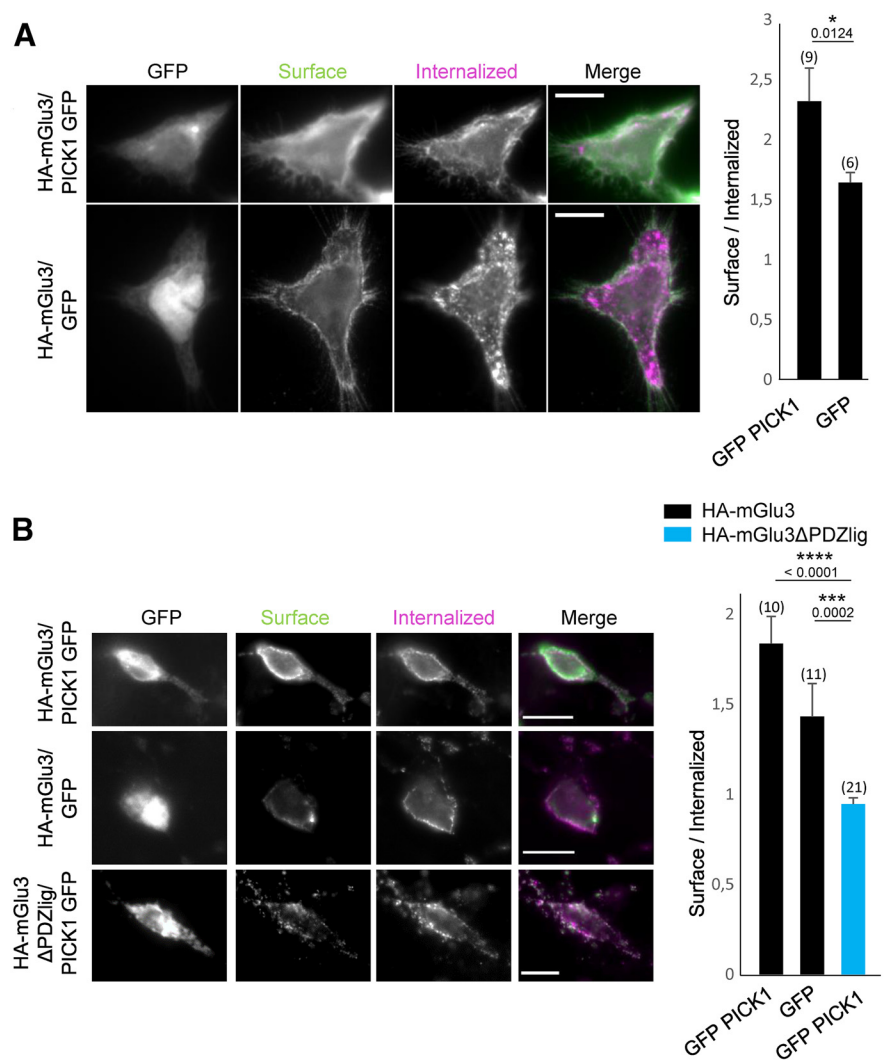


**Figure 4.** mGlu3 receptor internalization is regulated by PICK1. **A**, HEK-293 cells expressing WT mGlu3 receptor in the presence or absence of PICK1. mGlu3 receptors were labeled with an anti-HA antibody (pink represents internalized proteins; green represents surface-expressed receptor). Summary histogram quantifying the internalization of mGlu3 receptors. **B**, Hippocampal neurons were transiently cotransfected with HA-mGlu3 and GFP-PICK1 or with HA-mGlu3 $\Delta$ PDZlig and GFP-PICK1. Summary histogram quantifying internalization of mGlu3 receptors. Data are mean  $\pm$  SEM. \* $p < 0.05$ . \*\*\*\* $p < 0.0001$ . Scale bars, 10  $\mu\text{m}$ .

previously reported (Ster et al., 2011), the activation of mGlu3 receptors by LCCG-1 ( $10 \mu\text{M}$ ) induced a significant inward current in CA3 PCs, which is obvious under conditions of synaptic transmission block (TTX/D-AP5/picrotoxin; Fig. 7A). The LCCG-1-induced inward current was blocked in the presence of TAT-mGlu3 ( $10 \mu\text{M}$ , incubation 1 h/ $1 \mu\text{M}$  intracellular medium;  $-6.63 \pm 2.89 \text{ pA}$ , \* $p < 0.01$ , Fig. 7A,B) in CA3 PCs as well as in interneurons ( $-2.1 \pm 1.86 \text{ pA}$ , \*\* $p < 0.01$ , Fig. 7C). The TAT-control peptide had no effect in PCs ( $10 \mu\text{M}$ , 1 h incubation/ $1 \mu\text{M}$  intracellular medium, CA3 PCs: control =  $-23.29 \pm 1.00 \text{ pA}$ , TAT-control =  $-23.86 \pm 3.56 \text{ pA}$ ) and interneurons (CA3 interneuron: control =  $-21.75 \pm 4.60 \text{ pA}$ , TAT-control =  $-15 \pm 1.93 \text{ pA}$ ; Fig. 7A–C). Similar results were obtained in the presence of the PDZ domain inhibitor FSC231: the LCCG-1-induced inward current was blocked in CA3 PCs and interneurons (PCs: DMSO =  $-27.00 \pm 4.40 \text{ pA}$ , FSC231 =  $5.86 \pm 3.48 \text{ pA}$ , \*\* $p < 0.01$ ; CA3 interneurons: DMSO =  $-20.76 \pm 5.66 \text{ pA}$ , FSC231 =  $2.10 \pm 2.00 \text{ pA}$ , \*\* $p < 0.01$ ; Fig. 7A–C). Moreover, the spontaneous synaptic activity is not altered by treatment with the TAT peptides, suggesting that AMPA function is preserved (Fig. 7D; control =



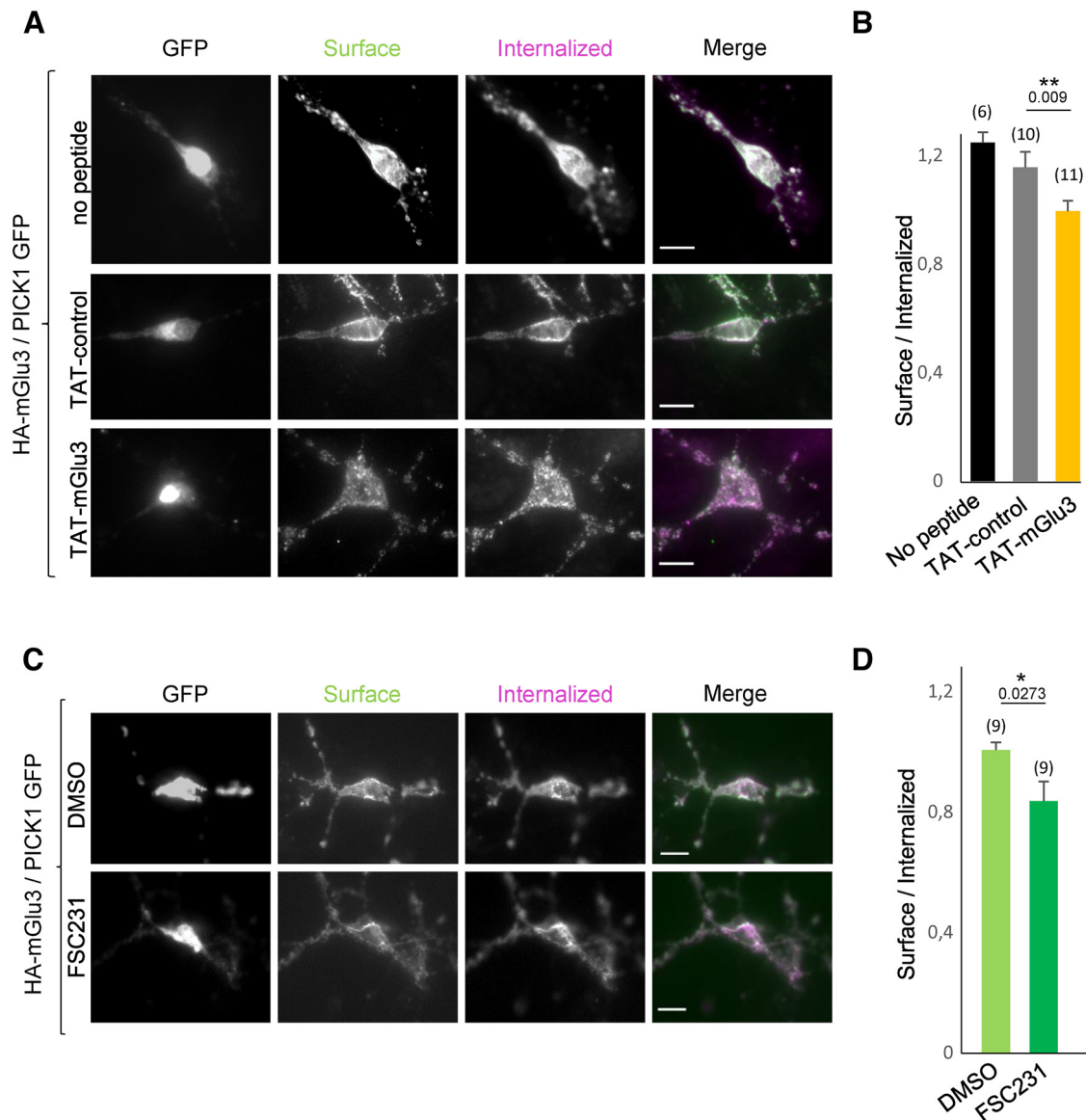


**Figure 5.** Effect of the TAT-mGlu3 peptide or FSC231 on the cell surface localization of mGlu3 receptors. **A, C**, Hippocampal neurons were transiently cotransfected with HA-mGlu3 and PICK1. **B** and **D**, Summary histograms quantify the internalization ratio from **A** and **C**, respectively. Neurons were treated with DMSO alone, FSC231 (25  $\mu$ M), TAT-mGlu3 (10  $\mu$ M), or TAT-control (10  $\mu$ M) peptides at 37°C for 1 h. Then neurons were labeled with anti-HA antibody, washed, and returned to conditioned media containing the same treatment at 37°C for 15 min. The cells were stained and images acquired as described in Figure 4. Scale bar, 10  $\mu$ m. **C**, Summary histogram quantifies the internalization ratio from **A** and **B**. Data are mean  $\pm$  SEM. \* $p$  < 0.05.

$-28.34 \pm 4.83$  pA, TAT-control =  $-24.12 \pm 5.33$  pA; TAT-mGlu3 =  $-25.26 \pm 3.98$  pA).

### Theta oscillations in the CA3 area of the hippocampus are altered by impairing the mGlu3-PICK1 interaction

Cholinergic activation of CA3 network in the hippocampus results in cycles of rhythmicity (Fischer et al., 1999; Buzsáki, 2002). The mGlu3-dependent inward current contributes to the theta oscillations in hippocampal organotypic slices (Ster et al., 2011). As we have shown that this current is also dependent on PICK1 binding to the receptor (Fig. 7), we hypothesized that the mGlu3-PICK1 complex could modulate the hippocampal network activity. Methacholine (the muscarinic receptor agonist) induces synaptic theta activity in CA3 PCs of hippocampal slice cultures (Fischer et al., 1999). Theta oscillations were induced in organotypic hippocampal slices by applying 500 nM MCh (20 min; frequency =  $12.9 \pm 0.38$  Hz, episodes/min =  $10.8 \pm 2.60$ )

(Fischer et al., 2002). The frequency of theta oscillations was significantly reduced in the presence of the TAT-mGlu3 peptide compared with TAT-control (frequency: TAT-mGlu3 =  $9.97 \pm 0.42$  Hz, TAT-control =  $12.64 \pm 0.75$  Hz,  $n = 6$ , \*\* $p$  < 0.01; Fig. 8A,B). A similar reduction in theta frequency was observed when applying FSC231 (frequency: DMSO =  $14.15 \pm 0.64$ , DMSO/FSC231 =  $10.54 \pm 1.11$ , \* $p$  < 0.05; Fig. 8A,B). The occurrence of theta episodes was not significantly altered in the presence of these treatments (episodes/min: TAT-mGlu3 =  $11.40 \pm 2.60$ , TAT-control =  $10.33 \pm 1.67$ ; DMSO =  $11 \pm 4.44$ , DMSO/FSC231 =  $7.8 \pm 1.98$ ; Fig. 8C). Hippocampal slice cultures respond to MCh by generating a high level of spontaneous synaptic activity that oscillates at theta frequencies. Analysis of spontaneous synaptic activity shows no significant difference in the amplitude of synaptic responses (EPSCs, IPSCs) during theta activity between TAT conditions (EPSCs: No peptide =  $-48.80 \pm 13.21$  pA; TAT-control =  $-55.67 \pm 18.13$  pA, TAT-mGlu3 =

–40.94 ± 7.38 pA; IPSCs: No peptide = –53.06 ± 14.79 pA; TAT-control = 53.55 ± 19.56 pA, TAT-mGlu3 = 58.32 ± 12.37 pA; Fig. 8D). Together, these results suggest the following: (1) a contribution of mGlu3-PICK1 to hippocampal theta oscillations (HTOs) in CA3 area and (2) no role in the generation of hippocampal theta rhythms.

### Effect of TAT-mGlu3 peptide on theta rhythms during sleep/wake states

During REM sleep and wake periods of increased attention in mice and rat, theta oscillations are observed in local field potential recordings from cortical structures, including the hippocampus (Robinson et al., 1977; Buzsaki, 2002). We asked what is the impact of the mGlu3-PICK1 complex on theta rhythms during sleep/wake states *in vivo*. We performed EEG recordings in mice injected with the TAT peptides via a cannula placed in the lateral ventricle. We confirmed the diffusion of the peptides in the hippocampus by detecting a fluorescent TAMRA-tagged version of TAT-mGlu3 35 min after injection (Fig. 9A). No peptide was detected in other regions, including the cortex. We tested the effect of the TAT-mGlu3 during sleep/wake states in freely behaving mice. By using a sleep scoring procedure based on movement detection and EMG signal analysis, we distinguished three different states: wake, NREM sleep, and REM sleep (Fig. 9B). Two-way ANOVA revealed significant alteration in low-frequency EEG power in the presence of the TAT peptides ( $F_{(2,266)} = 5.510$ ,  $p = 0.0045$ ). We focused on the period between 10 and 35 min after injection as the optimal time for peptide diffusion (Bertaso et al., 2008). The injection of TAT-mGlu3 resulted in significant reduction of REM sleep theta power measured in the dorsal hippocampal CA3 area (Fig. 9B; relative power low theta: baseline =  $3.33 \pm 0.33$ , post TAT-control =  $3.45 \pm 0.15$ , post TAT-mGlu3 =  $2.25 \pm 0.18$ ; relative power high theta: baseline =  $1.24 \pm 0.09$ , post TAT-control =  $1.52 \pm 0.19$ , post TAT-mGlu3 =  $0.97 \pm 0.07$ ). A decrease of theta power was also observed during NREM sleep (Fig. 9B; relative power low theta: baseline =  $2.59 \pm 0.12$ , post TAT-control =  $2.35 \pm 0.36$ , post TAT-mGlu3 =  $1.96 \pm 0.15$ ; relative power high theta: baseline =  $1.35 \pm 0.15$ , post TAT-control =  $1.4 \pm 0.2$ , post TAT-mGlu3 =  $1 \pm 0.16$ ) and wake states. No other frequency band was affected and the spectra profile returned to the baseline <1 h after peptide injection. The TAT-control peptide had no detectable effect on the EEG recordings.

### Discussion

In this study, we demonstrated that the PDZ ligand domain-containing mGlu3 receptor interacts with PICK1 and that this domain is required for their physical and functional interactions both *in vitro* and *in vivo*. In addition, we showed that such

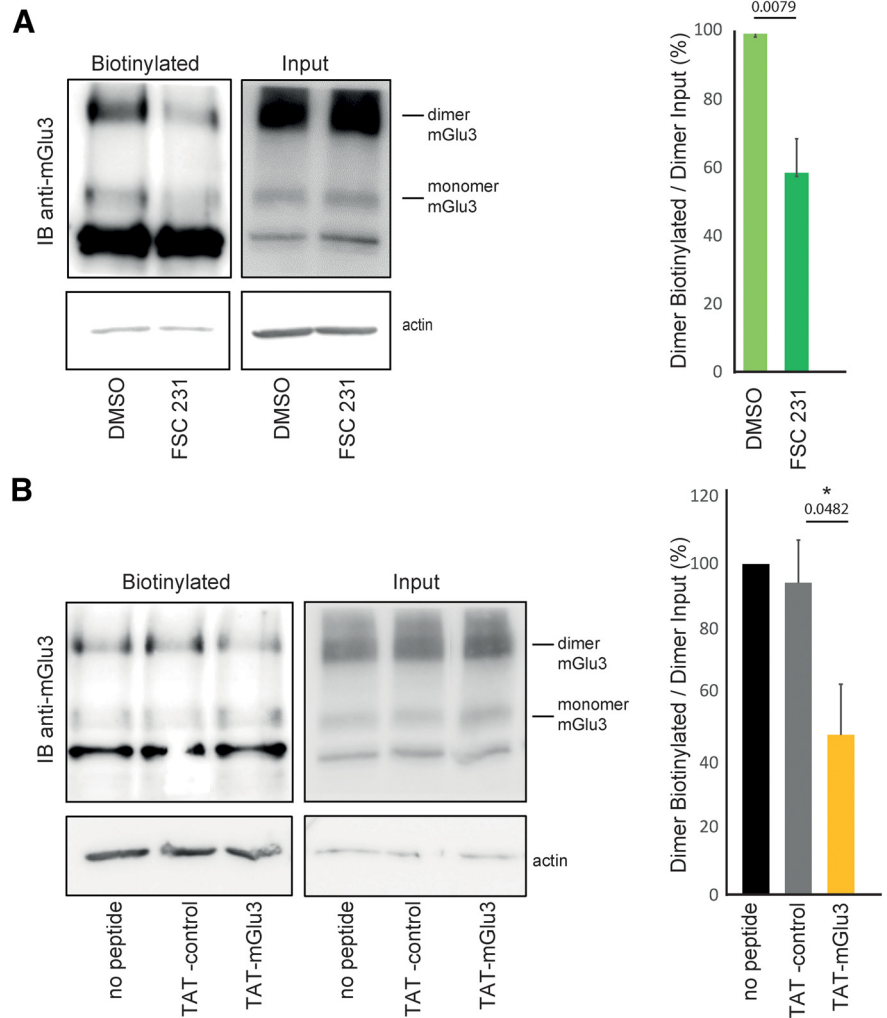


**Figure 6.** Cell-surface biotinylation of mGlu3 is modulated by the TAT-mGlu3 peptide or FSC231. **A**, Cell-surface biotinylation shows a decrease in mGlu3 receptor surface expression by using FSC231 (25  $\mu$ M, 30 min) compared with the DMSO control. No changes were found in the total mGlu3 receptor protein amount (Input). Densitometric quantification of Western blots of mGlu3 receptor surface biotinylation (right). Data are mean  $\pm$  SEM ( $n = 4$ ). **B**, TAT-control (10  $\mu$ M, 1 h incubation) shows no effect on mGlu3 receptor surface expression compared with the TAT-mGlu3 (10  $\mu$ M, 1 h incubation), which significantly decreases mGlu3 receptor surface expression. TAT-peptide treatments show no effect on mGlu3 receptor amount. Densitometric quantification of Western blots on mGlu3 receptor surface biotinylation (right). Data are mean  $\pm$  SEM ( $n = 4$ ). \* $p < 0.05$ .

interaction contributes to the targeting of receptors into the surface membrane of postsynaptic neurons, and significantly modulates the hippocampal network activity *in vitro* and *in vivo*.

### The functional significance of the specific interaction of mGlu3 receptor and PICK1

Protein interactions mediated by PDZ domains show great versatility, as PDZ domains bind to small C-terminal peptides (through Class I, II, and III binding motifs), internal protein segments, other PDZ domains, or even lipids (Nourry et al., 2003). mGlu2 and mGlu3 receptors possess the same and common (S/T)x(V/L) motif “SSL” that belongs to the Class I PDZ binding motifs. Yet, only the mGlu3 receptor binds to PICK1 as confirmed by our coimmunoprecipitation experiments, where PICK1 binds specifically to mGlu3 receptor and not the closely related mGlu2 receptor. The interaction between mGlu3 and PICK1 is disturbed by a TAT-mGlu3 peptide, which allows to distinguish the functions performed specifically by mGlu3 versus mGlu2. Therefore, a sequence of mGlu3 receptor outside its PDZ binding

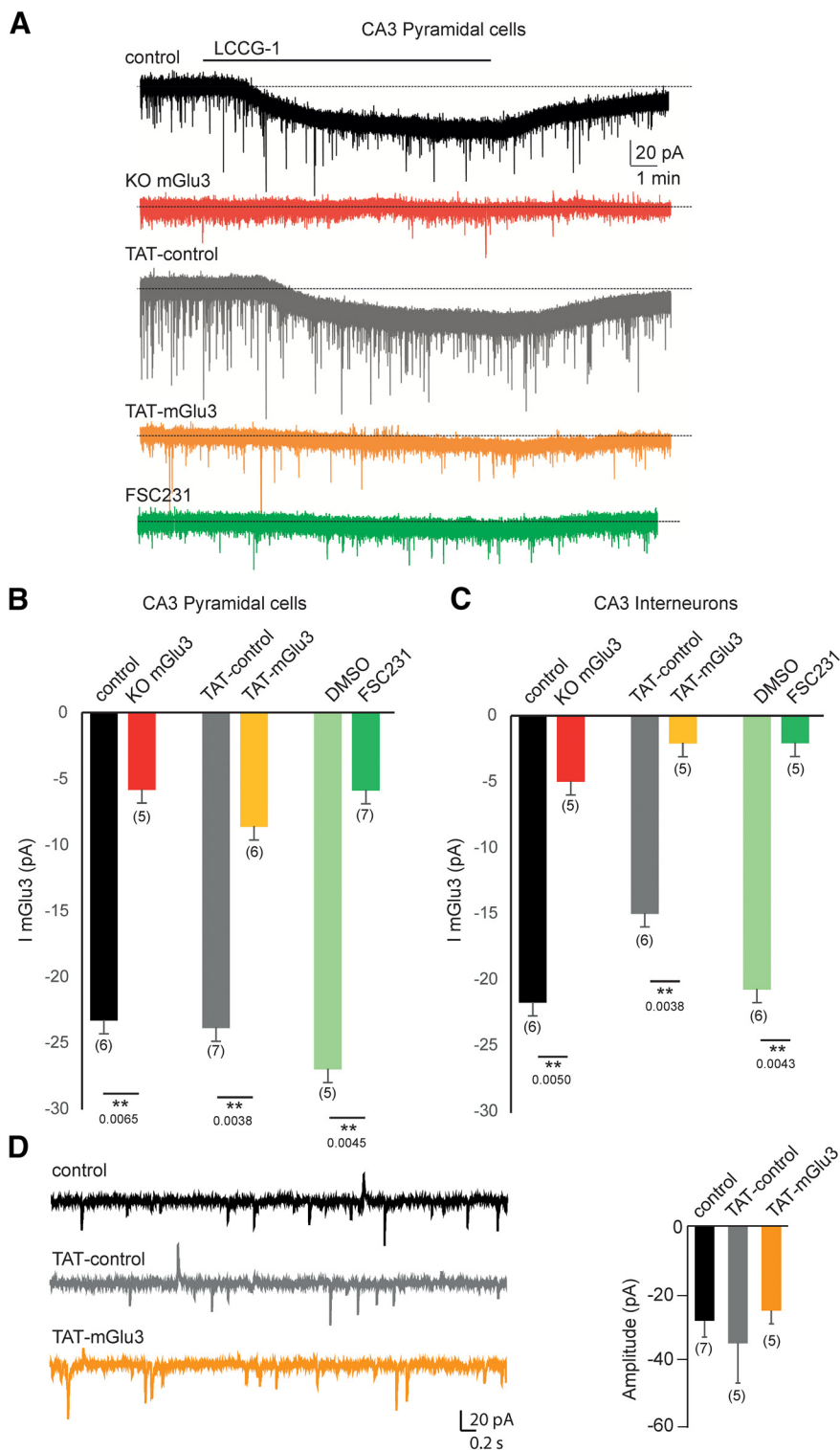


**Figure 7.** TAT-mGlu3 peptide or FSC231 disrupts the functional mGlu3 receptor in hippocampal organotypic slices. **A**, Bath application of the LCCG1 in the presence of TTX ( $1 \mu\text{M}$ ), picrotoxin ( $100 \mu\text{M}$ ), and D-AP5 ( $40 \mu\text{M}$ ) induces inward current in voltage-clamped CA3 PCs with or without TAT-control (gray trace and black trace, respectively). The inward current is not detected in CA3 PCs in the presence of TAT-mGlu3 peptide (orange trace) or FSC231 (dark green trace). Histograms represent the mean I mGlu3 current to illustrate the effect of TAT-mGlu3 peptides or FSC231 in PCs (**B**) and in interneurons (**C**). **D**, Representative activity recorded in a CA3 PCs (voltage-clamped at  $-70 \text{ mV}$ ) in the presence of TAT-mGlu3 peptides. Data are mean  $\pm$  SEM. \*\* $p < 0.01$ .

motif could contribute to the specificity of interaction with PICK1. Intriguingly, the total deletion of the last three amino acids corresponding to the PDZ-ligand domain of mGlu3 (mGlu3 $\Delta$ PDZlig) impairs the interaction with PICK1, whereas a

point of mutation of the last amino acid of the PDZ motif of mGlu3 receptors only reduces this interaction suggesting that the entire PDZ binding motif of mGlu3 receptor is required.

Protein–receptor interactions influence signal transduction mechanisms, trafficking, and localization of the receptor proteins (Xiao et al., 2000; Kim and Sheng, 2004). A large number of studies have established the importance of PDZ domain-mediated interactions in the localization and compartmentalization of several receptors and channels (Sheng and Wyszynski, 1997). To date, little is known about the molecular factors that govern the regulatory mechanisms associated with cell surface expression of mGlu3 receptors. Proteins that specifically interact with the PDZ ligand domain of mGlu3 receptor have not been clearly characterized. Removal of the PDZ ligand on mGlu3 receptor or absence of PICK1 in cultured transfected neurons considerably reduces surface localization of mGlu3 receptor, indicating that mGlu3–PICK1 interaction regulates receptor surface expression. These findings confirmed a key role for PICK1 in synaptic regulation, by adding the mGlu3 receptor to the list of its interacting partners. Indeed, in the brain, PICK1 is expressed in both the presynaptic and postsynaptic elements, where it serves different roles. For example, PICK1 is a key regulator of postsynaptic GluA2 AMPAR during plasticity (Kim et al., 2001; Steinberg et al., 2006). At the presynapse, PICK1 regulates the synaptic localization and function of the mGlu7 receptor and of dopamine and norepinephrine transporters (Torres et al., 2001; Perroy et al., 2002). Our electrophysiological data support the notion that postsynaptic mGlu3 receptors and PICK1 form a functional protein complex at the neuronal surface. Using the TAT-mGlu3 peptide, designed to disturb the endogenous interaction between mGlu3 and PICK1, we observed a decrease (40%–50% reduction) in membrane expression of mGlu3 receptors. However, we detected an almost complete reduction of the mGlu3 current. Several reasons could explain this apparent discrepancy. In Figure 5 we are working with cells that overexpress mGlu3 and PICK1, while in Figure 7 we used organotypic slices (i.e., endogenous proteins). The effect of the peptides could be strongly influenced by the amount of PICK1 that needs to be displaced from the receptor. In native conditions, PICK1 is not in excess compared with other mGlu3 binding partners. One



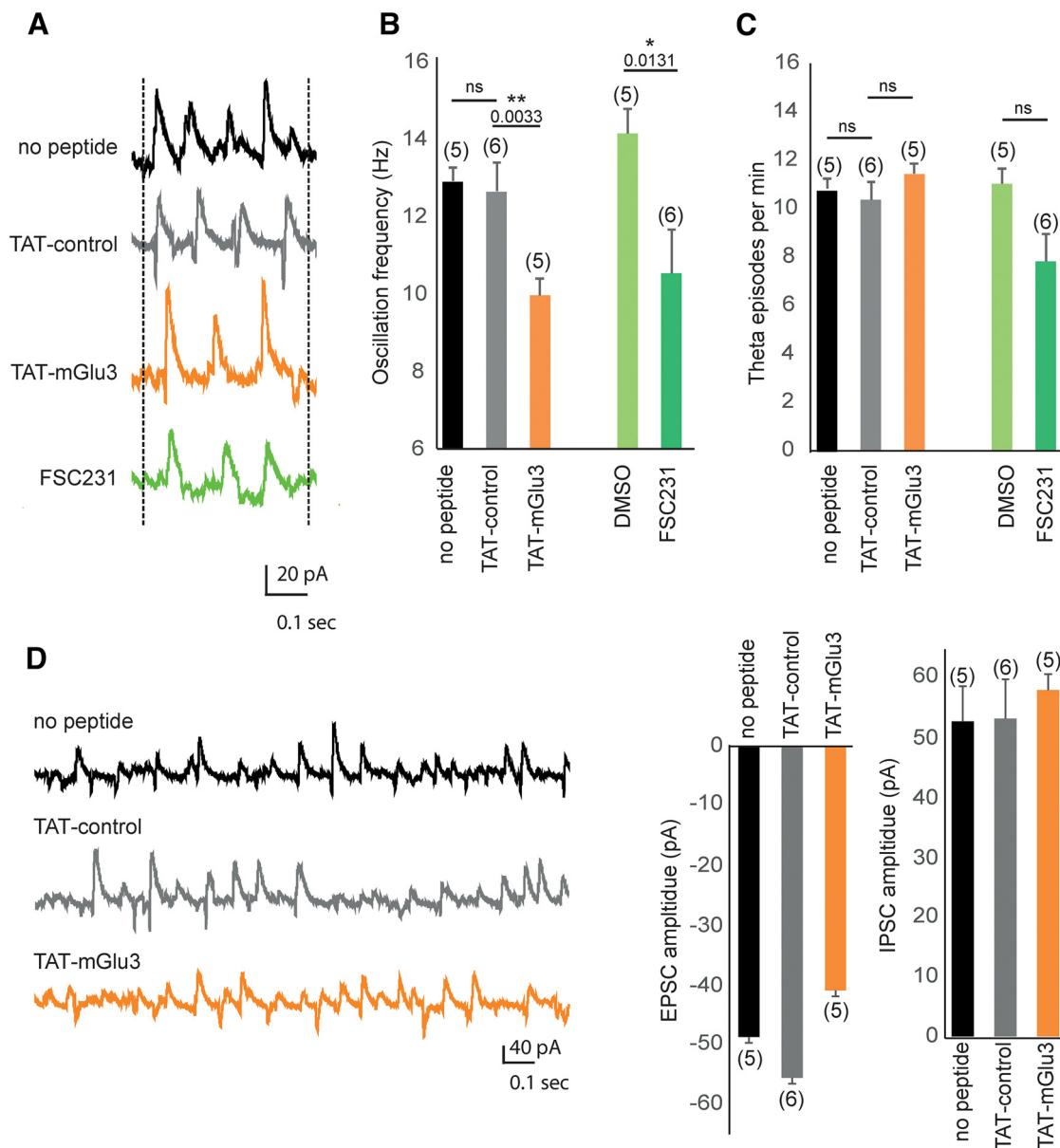


**Figure 8.** Methacholine-induced oscillations in the CA3 network are altered when PICK1 binding to mGlu3 is disrupted. **A**, Methacholine (500 nM; 10–20 min) induces synaptic theta activity in CA3 PCs of hippocampal slice cultures (Fischer et al., 1999). Representative traces of methacholine-induced theta oscillation recorded in CA3 PCs voltage-clamped at  $-70$  mV in control condition (black trace) and in the presence of TAT-control (gray trace), TAT-mGlu3 (orange trace), or FSC231 (green trace). **B**, Theta frequency was significantly decreased by the incubation with TAT-mGlu3 ( $10 \mu\text{M}$ , 1 h incubation), but not by the incubation of TAT-control. The FSC231 ( $25 \mu\text{M}$ , 30 min) also reduced the theta frequency similarly to the TAT-mGlu3. **C**, The occurrence of theta episodes was not altered in the presence of TAT-mGlu3 or FSC231 nor in the presence of TAT-control or DMSO. **D**, Representative spontaneous synaptic activity recorded in CA3 PCs (voltage-clamped at  $-70$  mV) in the presence of TAT-mGlu3 peptides. Data are mean  $\pm$  SEM. \* $p < 0.05$ . \*\* $p < 0.01$ .

could imagine that membrane localization could be affected partially by the disruption of PICK1 binding over other partners. On the other hand, the mGlu3 current (I mGlu3) could be more strongly dependent (and we could argue, completely dependent) on PICK1 binding and signaling; therefore, disruption of the complex would lead to a total wipe out of the current. These data suggest that the alteration of the mGlu3-PICK1 interaction reduces functional mGlu3 receptors at the neuronal cell surface and point to the physiological relevance for the interaction of postsynaptic mGlu3 receptor and PICK1.

Our data do not exclude an interaction of the two proteins at the presynaptic site, where it could potentially modulate the excitatory/inhibitory neurotransmitter release.

Likewise, we cannot rule out the possibility that PICK1 could also influence and/or participate to mGlu3 signal transduction mechanisms, as it does for other glutamate receptors, including GluA2 and mGlu7 (Kim et al., 2001; Perroy et al., 2002). PICK1 bind PKC  $\alpha$ -subunit and mGlu3 receptors could signal through activation of a PLC-PKC-dependent pathway (Rosenberg et al., 2016). Additional investigation of such molecular mechanisms would be interesting.

#### The physiological relevance of the mGlu3-PICK1 complex

HTOs are prominent local field potentials occurring in the 4–14 Hz frequency range and generated essentially by the hippocampus (Buzsáki, 2002). Increasing evidence implicates Group II mGluRs in HTO both *in vitro* and *in vivo* (Feinberg et al., 2005;

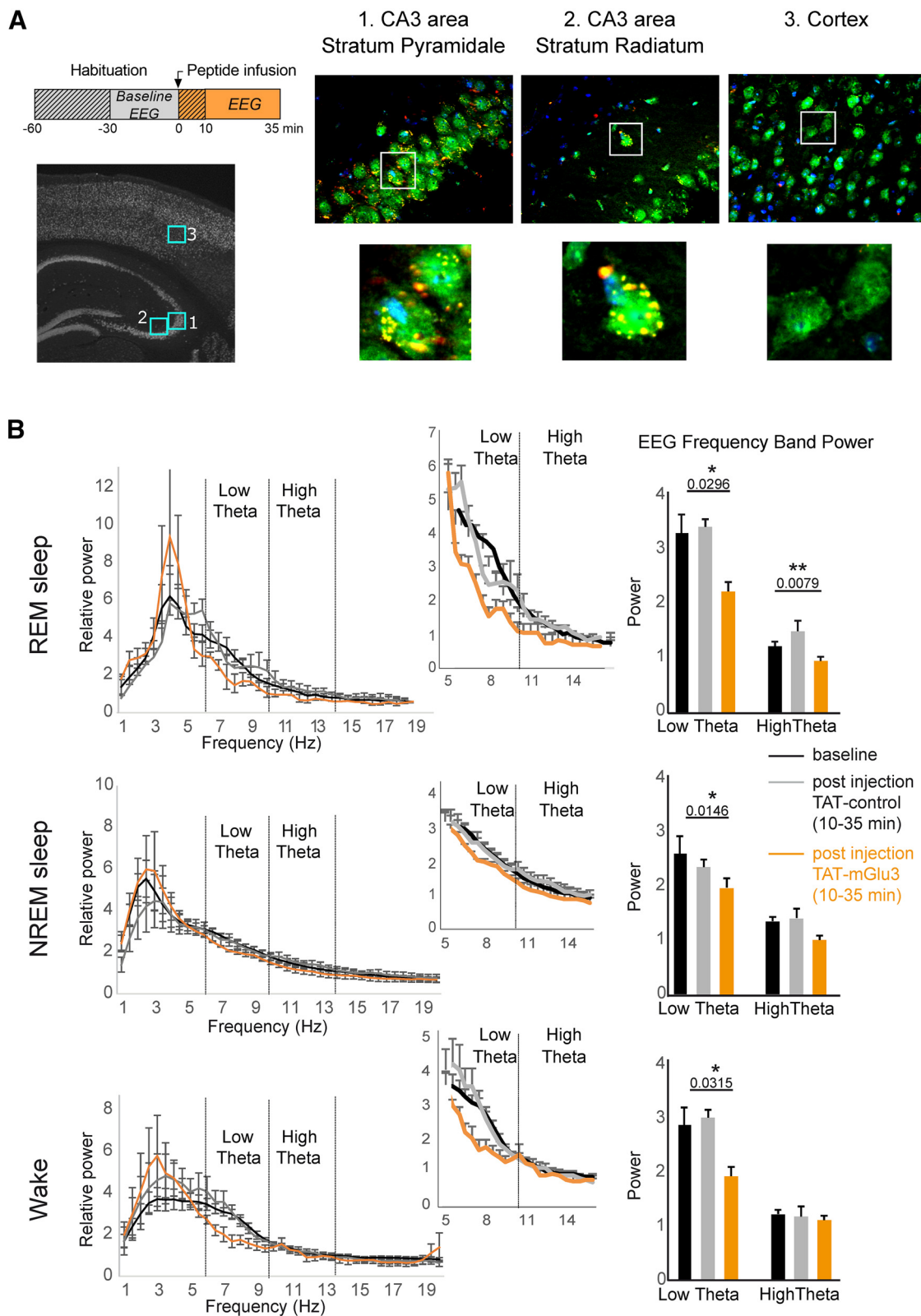


**Figure 9.** Effect of TAT-mGlu3 peptide on theta rhythms during sleep and wake states. **A**, TAT-mGlu3 TAMRA peptide was injected into the ventricle of C57Bl6/J adult mice and visualized by immunohistochemistry. TAMRA expression (red) was detected in hippocampal cells but not in the cortex (green represents neuronal marker NeuN; blue represents nuclear marker DAPI). **B**, Effect of intraventricular injection of the TAT-control or TAT-mGlu3 peptides (5  $\mu$ l, 500  $\mu$ M, 750 nl/ml) on the power spectrum during REM sleep, NREM sleep, and wake ( $n = 5$ ). Middle panels, Zoom on theta frequencies. Right panels, Sum of low and theta frequency power. Data are mean  $\pm$  SEM. \* $p < 0.05$ . \*\* $p < 0.001$ .

Ster et al., 2011; Ahnaou et al., 2014). Modulation of mGlu2 and mGlu3 receptors influences theta oscillations *in vivo* using different rat strains (Wood et al., 2018). We have examined whether disrupting the mGlu3-PICK1 complex could affect theta rhythms. In organotypic hippocampal slices, Mch-mediated theta oscillations are decreased by treatment with the TAT-mGlu3 peptide and the PICK1 binding molecule, FSC231. *In vivo*, theta oscillations are most prominent during wake periods of increased attention and REM sleep (Buzsaki, 2002). mGlu2/3-modulating drugs (agonist, antagonist) profoundly influence theta oscillation, suggesting involvement of both receptor types in the control of theta oscillations (Feinberg et al., 2002, 2005; Siok et al., 2012; Ahnaou et al., 2014; Wood et al., 2018). Indeed, pharmacological studies using orthosteric compounds have suggested the involvement of mGlu2/3 receptors in oscillatory activity, with reduction of theta oscillations by mGlu2/3 agonism (Feinberg et al., 2002; Jones et al., 2012) and an activation of the same oscillations following mGlu2/3 antagonism (Feinberg et al., 2005; Ahnaou et al., 2014). Unfortunately, currently available orthosteric compounds act on both mGlu2 and mGlu3 subtypes. Thus, to clarify the specific function of each receptor, studies in KO mice have been useful to distinguish the role of mGlu2 and mGlu3 receptors. However, some mixed results have been observed, possibly related to their genetic background and compensatory expression (Higgins et al., 2004; Lyon et al., 2011; Ahnaou et al., 2014; De Filippis et al., 2015). Thus, at present, it is not easy to determine the role of mGlu3 or mGlu2 specifically/independently in theta oscillations. However, our study shows a major role of mGlu3 receptors in theta rhythms via the specific interaction between mGlu3 and PICK1 (not mGlu2) and suggests a completely different effect of mGlu3 (compared with mGlu2) receptors on HTOs.

In freely moving mice, we observed a significant reduction of the theta frequency power during REM sleep, NREM sleep, and wake states on intracerebral injection of the TAT-mGlu3 peptide. HTO controls the timing of activity across neuronal populations in the hippocampus, PFC, and amygdala and coordinate  $\gamma$  oscillatory activity. Consequently, theta oscillations are suggested to be important in cognitive functions (Basar et al., 2001; Jones and Wilson, 2005). Thus, even small changes in baseline HTO frequencies during REM sleep and quiet waking are likely to alter neural activity across large distributed brain networks, ultimately generating modifications in behavioral processes. Our data suggest that alteration of mGlu3-PICK1 interaction modifies HTO during sleep/wake states and could predict a deficit in learning rates.

### Opening on schizophrenia

Disruption of neural oscillations and synchrony may play an important role in the pathophysiology of schizophrenia, a neurodevelopmental disorder marked by abnormalities in sensory processing and cognition. Although recent research is primarily focusing on high-frequency oscillations, there is also evidence of disturbances in slow rhythms in the  $\delta$  and theta bands in schizophrenia (Koenig et al., 2001; Ford et al., 2002; Basar-Eroglu et al., 2008; Bates et al., 2009). To date, Group II mGluRs draw a great interest as targets to treat such psychiatric conditions (Maksymetz et al., 2017). Identification of new proteins that associate specifically to mGlu3 receptors will advance our understanding of the regulatory mechanisms associated with their targeting and function

and ultimately might provide new therapeutic strategies to counter these psychiatric conditions.

### References

- Ahnaou A, Ver Donck L, Drinkenburg WH (2014) Blockade of the metabotropic glutamate (mGluR2) modulates arousal through vigilance states transitions: evidence from sleep-wake EEG in rodents. *Behav Brain Res* 270:56–67.
- Ango F, Pin JP, Tu JC, Xiao B, Worley PF, Bockaert J, Fagni L (2000) Dendritic and axonal targeting of type 5 metabotropic glutamate receptor is regulated by homer1 proteins and neuronal excitation. *J Neurosci* 20:8710–8716.
- Basar E (2013) Brain oscillations in neuropsychiatric disease. *Dialogues Clin Neurosci* 15:291–300.
- Basar E, Basar-Eroglu C, Karakas S, Schürmann M (2001) Gamma, alpha, delta, and theta oscillations govern cognitive processes. *Int J Psychophysiol* 39:241–248.
- Basar-Eroglu C, Schmiedt-Fehr C, Marbach S, Brand A, Mathes B (2008) Altered oscillatory alpha and theta networks in schizophrenia. *Brain Res* 1235:143–152.
- Bates AT, Kiehl KA, Laurens KR, Liddle PF (2009) Low-frequency EEG oscillations associated with information processing in schizophrenia. *Schizophr Res* 115:222–230.
- Berry S, Weinmann O, Fritz AK, Rust R, Wolfer D, Schwab ME, Gerber U, Ster J (2018) Loss of Nogo-A, encoded by the schizophrenia risk gene *Rtn4*, reduces mGlu3 expression and causes hyperexcitability in hippocampal CA3 circuits. *PLoS One* 13:e0200896.
- Bertaso F, et al. (2008) PICK1 uncoupling from mGluR7a causes absence-like seizures. *Nat Neurosci* 11:940–948.
- Bockaert J, Perroy J, Becamel C, Marin P, Fagni L (2010) GPCR interacting proteins (GIPs) in the nervous system: roles in physiology and pathologies. *Annu Rev Pharmacol Toxicol* 50:89–109.
- Boudin H, Doan A, Xia J, Shigemoto R, Haganir RL, Worley P, Craig AM (2000) Presynaptic clustering of mGluR7a requires the PICK1 PDZ domain binding site. *Neuron* 28:485–497.
- Bruno V, Caraci F, Copani A, Matrisciano F, Nicoletti F, Battaglia G (2017) The impact of metabotropic glutamate receptors into active neurodegenerative processes: a ‘dark side’ in the development of new symptomatic treatments for neurologic and psychiatric disorders. *Neuropharmacology* 115:180–192.
- Buzsaki G (2002) Theta oscillations in the hippocampus. *Neuron* 33:325–340.
- Buzsaki G, Draguhn A (2004) Neuronal oscillations in cortical networks. *Science* 304:1926–1929.
- Corti C, Crepaldi L, Mion S, Roth AL, Xuereb JH, Ferraguti F (2007) Altered dimerization of metabotropic glutamate receptor 3 in schizophrenia. *Biol Psychiatry* 62:747–755.
- Coyle JT (2012) NMDA receptor and schizophrenia: a brief history. *Schizophr Bull* 38:920–926.
- De Filippis B, Lyon L, Taylor A, Lane T, Burnet PW, Harrison PJ, Bannerman DM (2015) The role of Group II metabotropic glutamate receptors in cognition and anxiety: comparative studies in *GRM2(-/-)*, *GRM3(-/-)* and *GRM2/3(-/-)* knockout mice. *Neuropharmacology* 89:19–32.
- Dubois F, Vandermoere F, Gernez A, Murphy J, Toth R, Chen S, Geraghty KM, Morrice NA, MacKintosh C (2009) Differential 14-3-3 affinity capture reveals new downstream targets of phosphatidylinositol 3-kinase signaling. *Mol Cell Proteomics* 8:2487–2499.
- Feinberg I, Campbell IG, Schoepp DD, Anderson K (2002) The selective group mGlu2/3 receptor agonist LY379268 suppresses REM sleep and fast EEG in the rat. *Pharmacol Biochem Behav* 73:467–474.
- Feinberg I, Schoepp DD, Hsieh KC, Darchia N, Campbell IG (2005) The metabotropic glutamate (mGlu)2/3 receptor antagonist LY341495 [2S-2-amino-2-(1S,2S-2-carboxycyclopropyl-1-yl)-3-(xanth-9-yl)propanoic acid] stimulates waking and fast electroencephalogram power and blocks the effects of the mGlu2/3 receptor agonist ly379268 [(-)-2-oxa-4-aminobicyclo[3.1.0]hexane-4,6-dicarboxylate] in rats. *J Pharmacol Exp Ther* 312:826–833.
- Fischer Y, Gähwiler BH, Thompson SM (1999) Activation of intrinsic hippocampal theta oscillations by acetylcholine in rat septo-hippocampal cultures. *J Physiol* 519:405–413.



- Fischer Y, Wittner L, Freund TF, Gahwiler BH (2002) Simultaneous activation of gamma and theta network oscillations in rat hippocampal slice cultures. *J Physiol* 539:857–868.
- Flajole M, Rakhilin S, Wang H, Starkova N, Nuangchamnong N, Nairn AC, Greengard P (2003) Protein phosphatase 2C binds selectively to and dephosphorylates metabotropic glutamate receptor 3. *Proc Natl Acad Sci USA* 100:16006–16011.
- Ford JM, Mathalon DH, Whitfield S, Faustman WO, Roth WT (2002) Reduced communication between frontal and temporal lobes during talking in schizophrenia. *Biol Psychiatry* 51:485–492.
- Gandal MJ, Edgar JC, Klook K, Siegel SJ (2012) Gamma synchrony: towards a translational biomarker for the treatment-resistant symptoms of schizophrenia. *Neuropharmacology* 62:1504–1518.
- Higgins GA, Ballard TM, Kew JN, Richards JG, Kemp JA, Adam G, Woltering T, Nakanishi S, Mutel V (2004) Pharmacological manipulation of mGlu2 receptors influences cognitive performance in the rodent. *Neuropharmacology* 46:907–917.
- Hirbec H, Perestenko O, Nishimune A, Meyer G, Nakanishi S, Henley JM, Dev KK (2002) The PDZ proteins PICK1, GRIP, and syntenin bind multiple glutamate receptor subtypes: analysis of PDZ binding motifs. *J Biol Chem* 277:15221–15224.
- Joffe ME, Santiago CI, Engers JL, Lindsley CW, Conn PJ (2019) Metabotropic glutamate receptor subtype 3 gates acute stress-induced dysregulation of amygdalo-cortical function. *Mol Psychiatry* 24:916–927.
- Jones NC, Reddy M, Anderson P, Salzberg MR, O'Brien TJ, Pinault D (2012) Acute administration of typical and atypical antipsychotics reduces EEG gamma power, but only the preclinical compound LY379268 reduces the ketamine-induced rise in gamma power. *Int J Neuropsychopharmacol* 15:657–668.
- Jones MW, Wilson MA (2005) Theta rhythms coordinate hippocampal-frontal interactions in a spatial memory task. *PLoS Biol* 3:e402.
- Kim CH, Chung HJ, Lee HK, Hagan RL (2001) Interaction of the AMPA receptor subunit GluR2/3 with PDZ domains regulates hippocampal long-term depression. *Proc Natl Acad Sci USA* 98:11725–11730.
- Kim E, Sheng M (2004) PDZ domain proteins of synapses. *Nat Rev Neurosci* 5:771–781.
- Koenig T, Lehmann D, Saito N, Kuginuki T, Kinoshita T, Koukkou M (2001) Decreased functional connectivity of EEG theta-frequency activity in first-episode, neuroleptic-naive patients with schizophrenia: preliminary results. *Schizophr Res* 50:55–60.
- Lavezzi G, McCallum J, Dewey CM, Roche KW (2004) Subunit-specific regulation of NMDA receptor endocytosis. *J Neurosci* 24:6383–6391.
- Lea PM, Wroblewska B, Sarvey JM, Neale JH (2001)  $\beta$ -NAAG rescues LTP from blockade by NAAG in rat dentate gyrus via the type 3 metabotropic glutamate receptor. *J Neurophysiol* 85:1097–1106.
- Lisman J (2016) Low-frequency brain oscillations in schizophrenia. *JAMA Psychiatry* 73:298–299.
- Lyon L, Burnet PW, Kew JN, Corti C, Rawlins JN, Lane T, De Filippis B, Harrison PJ, Bannerman DM (2011) Fractionation of spatial memory in GRM2/3 (mGlu2/mGlu3) double knockout mice reveals a role for Group II metabotropic glutamate receptors at the interface between arousal and cognition. *Neuropsychopharmacology* 36:2616–2628.
- Madsen KL, Beuming T, Niv MY, Chang CW, Dev KK, Weinstein H, Gether U (2005) Molecular determinants for the complex binding specificity of the PDZ domain in PICK1. *J Biol Chem* 280:20539–20548.
- Maksymetz J, Moran SP, Conn PJ (2017) Targeting metabotropic glutamate receptors for novel treatments of schizophrenia. *Mol Brain* 10:15.
- Moutin E, Raynaud F, Roger J, Pellegrino E, Homburger V, Bertaso F, Ollendorff V, Bockaert J, Fagni L, Perroy J (2012) Dynamic remodeling of scaffold interactions in dendritic spines controls synaptic excitability. *J Cell Biol* 198:251–263.
- Moutin E, Hemonnot AL, Seube V, Linck N, Rassendren F, Perroy J, Compan V (2020) Procedures for culturing and genetically manipulating murine hippocampal postnatal neurons. *Front Synaptic Neurosci* 12:19.
- Moutin E, et al. (2021) Restoring glutamate receptor dynamics at synapses rescues autism-like deficits in Shank3-deficient mice. *Mol Psychiatry* 26:7596–7609.
- Nourry C, Grant SG, Borg JP (2003) PDZ domain proteins: plug and play! *Sci STKE* 2003:RE7.
- Olney JW, Labruyere J, Wang G, Wozniak DF, Price MT, Sesma MA (1991) NMDA antagonist neurotoxicity: mechanism and prevention. *Science* 254:1515–1518.
- Pelkey KA, Chittajallu R, Craig MT, Tricoire L, Wester JC, McBain CJ (2017) Hippocampal GABAergic inhibitory interneurons. *Physiol Rev* 97:1619–1747.
- Perroy J, Richard S, Nargeot J, Bockaert J, Fagni L (2002) Permissive effect of voltage on mGlu 7 receptor subtype signaling in neurons. *J Biol Chem* 277:1223–1228.
- Perroy J, Raynaud F, Homburger V, Rousset MC, Telley L, Bockaert J, Fagni L (2008) Direct interaction enables cross-talk between ionotropic and Group I metabotropic glutamate receptors. *J Biol Chem* 283:6799–6805.
- Robinson TE, Kramis RC, Vanderwolf CH (1977) Two types of cerebral activation during active sleep: relations to behavior. *Brain Res* 124:544–549.
- Rosenberg N, Gerber U, Ster J (2016) Activation of group II metabotropic glutamate receptors promotes LTP induction at Schaffer collateral-CA1 pyramidal cell synapses by priming NMDA receptors. *J Neurosci* 36:11521–11531.
- Rouse ST, Marino MJ, Bradley SR, Awad H, Wittmann M, Conn PJ (2000) Distribution and roles of metabotropic glutamate receptors in the basal ganglia motor circuit: implications for treatment of Parkinson's disease and related disorders. *Pharmacol Ther* 88:427–435.
- Sheng M, Wyszynski M (1997) Ion channel targeting in neurons. *Bioessays* 19:847–853.
- Siok CJ, Cogan SM, Shifflett LB, Doran AC, Kocsis B, Hajos M (2012) Comparative analysis of the neurophysiological profile of Group II metabotropic glutamate receptor activators and diazepam: effects on hippocampal and cortical EEG patterns in rats. *Neuropharmacology* 62:226–236.
- Sohal VS, Zhang F, Yizhar O, Deisseroth K (2009) Parvalbumin neurons and gamma rhythms enhance cortical circuit performance. *Nature* 459:698–702.
- Steinberg JP, Takamiya K, Shen Y, Xia J, Rubio ME, Yu S, Jin W, Thomas GM, Linden DJ, Hagan RL (2006) Targeted in vivo mutations of the AMPA receptor subunit GluR2 and its interacting protein PICK1 eliminate cerebellar long-term depression. *Neuron* 49:845–860.
- Ster J, Mateos JM, Grewe BF, Coiret G, Corti C, Corsi M, Helmchen F, Gerber U (2011) Enhancement of CA3 hippocampal network activity by activation of Group II metabotropic glutamate receptors. *Proc Natl Acad Sci USA* 108:9993–9997.
- Stoppini L, Buchs PA, Muller D (1991) A simple method for organotypic cultures of nervous tissue. *J Neurosci Methods* 37:173–182.
- Thorsen TS, et al. (2010) Identification of a small-molecule inhibitor of the PICK1 PDZ domain that inhibits hippocampal LTP and LTD. *Proc Natl Acad Sci USA* 107:413–418.
- Torres GE, Yao WD, Mohn AR, Quan H, Kim KM, Levey AI, Staudinger J, Caron MG (2001) Functional interaction between monoamine plasma membrane transporters and the synaptic PDZ domain-containing protein PICK1. *Neuron* 30:121–134.
- Trepanier C, Lei G, Xie YF, MacDonald JF (2013) Group II metabotropic glutamate receptors modify N-methyl-D-aspartate receptors via Src kinase. *Sci Rep* 3:926.
- Uhlhaas PJ, Singer W (2010) Abnormal neural oscillations and synchrony in schizophrenia. *Nat Rev Neurosci* 11:100–113.
- Wood CM, Wafford KA, McCarthy AP, Hewes N, Shanks E, Lodge D, Robinson ES (2018) Investigating the role of mGluR2 versus mGluR3 in antipsychotic-like effects, sleep-wake architecture and network oscillatory activity using novel Han Wistar rats lacking mGluR2 expression. *Neuropharmacology* 140:246–259.
- Xiao B, Tu JC, Worley PF (2000) Homer: a link between neural activity and glutamate receptor function. *Curr Opin Neurobiol* 10:370–374.
- Xu J, Xia J (2006) Structure and function of PICK1. *Neurosignals* 15:190–201.
- Yokoi M, et al. (1996) Impairment of hippocampal mossy fiber LTD in mice lacking mGluR2. *Science* 273:645–647.